

# Investigating the angular distribution of FCNC process $B_c \rightarrow D_s^*(\rightarrow D_s\pi)\ell^+\ell^-$

Yu-Shuai Li<sup>1,2,3,5\*</sup> and Xiang Liu<sup>1,2,3,4,5†</sup>

<sup>1</sup>*School of Physical Science and Technology, Lanzhou University, Lanzhou 730000, China*

<sup>2</sup>*Lanzhou Center for Theoretical Physics, Key Laboratory of Theoretical Physics of Gansu Province, Lanzhou University, Lanzhou 730000, China*

<sup>3</sup>*Key Laboratory of Quantum Theory and Applications of MoE, Lanzhou University, Lanzhou 730000, China*

<sup>4</sup>*MoE Frontiers Science Center for Rare Isotopes, Lanzhou University, Lanzhou 730000, China*

<sup>5</sup>*Research Center for Hadron and CSR Physics, Lanzhou University and Institute of Modern Physics of CAS, Lanzhou 730000, China*

In this work, we study the flavor-changing neutral-current process  $B_c \rightarrow D_s^*(\rightarrow D_s\pi)\ell^+\ell^-$  ( $\ell = e, \mu, \tau$ ). The relevant weak transition form factors are obtained by using the covariant light-front quark model, in which, the main inputs, i.e., the meson wave functions of  $B_c$  and  $D_s^*$ , are adopted as the numerical wave functions from the solution of the Schrödinger equation with the modified Godfrey-Isgur model. With the obtained form factors, we further investigate the relevant branching fractions and their ratios, and some angular observables, i.e., the forward-backward asymmetry  $A_{FB}$ , the polarization fractions  $F_{L(T)}$ , and the  $CP$ -averaged angular coefficients  $S_i$  and the  $CP$  asymmetry coefficients  $A_i$ . We also present our results of the clean angular observables  $P_{1,2,3}$  and  $P'_{4,5,6,8}$ , which can reduce the uncertainties from the form factors. Our results show that the corresponding branching fractions of the electron or muon channels can reach up to  $10^{-8}$ . With more data being accumulated in the LHCb experiment, our results are helpful for exploring this process, and deepen our understanding of the physics around the  $b \rightarrow s\ell^+\ell^-$  process.

## I. INTRODUCTION

The flavor-changing neutral-current (FCNC) process, like the  $b \rightarrow s\ell^+\ell^-$  ( $\ell=e, \mu, \tau$ ) we are concerned with, has attracted the attention of both theorists and experimentalists, and of course has been widely studied. The FCNC process is forbidden at the tree level, and can only operate through loop diagrams in the Standard Model (SM). At the lowest order, three amplitudes contribute to the decay width, i.e., the photo penguin diagram, the  $Z$  penguin diagram, and the  $W^+W^-$  box diagram. In all three diagrams, the virtual  $t$  quark plays a dominant role, while the  $c$  and  $u$  quarks are the secondary contributions. The FCNC process is very sensitive to the new physical effects. This suggests that it can serve as a perfect platform to search directly for new physics (NP) beyond the SM [1, 2].

The  $b \rightarrow s\ell^+\ell^-$  in bottom(-stranged) mesons sector is an attractive experimental topic. The experimental search of the FCNC processes  $B \rightarrow K^{(*)}\ell^+\ell^-$  started in 1998 [3–5]. The first observation of  $B \rightarrow K\ell^+\ell^-$  was made by the Belle Collaboration in 2001 with a statistical significance of 5.3 [6]. From 2001 to now, the  $B \rightarrow K^{(*)}\ell^+\ell^-$  with  $\ell^+\ell^-$  being either an  $e^+e^-$  or  $\mu^+\mu^-$  pair has been observed or measured by the Belle [6–11], the BABAR [12–14], the CDF [15], the CMS [16], and the LHCb collaborations [17–22]. In particular, the LHCb Collaboration measured the form-factor-independent observable  $P'_5$  [22], and found a 2.5 standard deviation ( $\sigma$ ) discrepancy to the SM prediction [23] after integrating over  $1.0 < q^2 < 6.0$  GeV<sup>2</sup>. In addition, the LHCb Collaboration recently reported the most precise measurement of the ratio of branching fractions for  $B^+ \rightarrow K^+\mu^+\mu^-$  and  $B^+ \rightarrow K^+e^+e^-$  decays in  $1.1 < q^2 < 6.0$  GeV<sup>2</sup> as  $R_K^{\mu e} = 0.846^{+0.044}_{-0.041}$  [21], indicating a 3.1

$\sigma$  discrepancy with the SM prediction [2, 24], and providing evidence for the violation of lepton flavor universality (LFU). For the  $B_s$  decays, there have been some experiments, such as the CDF [25, 26] and the DØ experiments [27], to search for the  $B_s \rightarrow \phi\ell^+\ell^-$  mode. In 2011, the  $B_s \rightarrow \phi\mu^+\mu^-$  mode was first observed in the CDF experiment [28], and then be measured by the CDF [15] and the LHCb collaborations [29–31]. The electron mode is still missing in the experiment. Moreover, in Ref. [31] the LHCb Collaboration also reported their measurement of the  $B_s \rightarrow f_2'(1525)\mu^+\mu^-$  process. Compared to the di-electronic and di-muonic modes, the di-tauic mode is less studied. There is a Belle experiment, which focused on the  $B^0 \rightarrow K^{*0}\tau^+\tau^-$  process, and determined the upper limit of the branching fraction  $\mathcal{B}(B^0 \rightarrow K^{*0}\tau^+\tau^-) < 3.1 \times 10^{-3}$  at 90% confidence level [32].

The FCNC decay of bottom(-stranged) mesons has also been studied by various theoretical approaches, such as the lattice QCD (LQCD) [33–35], the light-cone sum rule [36–42], the QCD factorization [43], the perturbative QCD (pQCD) [45–49] and its combination with LQCD data [50, 51], as well as various quark models [52–58], and so on [59, 60]. On the other hand, in order to understand the discrepancy of the value of  $R$  with the SM prediction, the effects beyond the SM are considered. Following this line of thought, the extensions of the SM via the extend Higgs-boson [61–65], supersymmetry [66, 67], and extra dimensions [68] have been used. At the same time, some NP models with an additional heavy neutral boson [69–81] or leptoquarks [82–97] were also considered.

Although great progress has been made both experimentally and theoretically in the rare semileptonic decays of bottom(-strange) mesons in recent decades, those of bottom-charmed mesons have been less studied. Compared to the  $B_{(s)}$  mesons, the  $B_c$  meson is difficult to produce at the Belle experiment because the  $B_c\bar{B}_c$  is close to 12.5 GeV, which is far from the energy region of  $\Upsilon(4S)$ . Moreover, according to  $f_c/f_u = (7.5 \pm 1.8) \times 10^{-3}$  measured by the LHCb Collabo-

\*Electronic address: liysh20@lzu.edu.cn

†Electronic address: xiangliu@lzu.edu.cn

ration [98], the  $B_c$  meson is also underproductivity in the  $pp$  experiment. Here, the  $f_c$  and  $f_u$  are the fragmentation fractions of  $B_c$  and  $B$  meson respectively in  $pp$  collisions. As a result, the  $B_c$  meson decay has received less experimental attentions in the past. However, with the high-luminosity upgrade of the Large Hadron Collider (LHC), this situation is likely to improve. Recently, the LHCb Collaboration reported the result of the  $B_c^+ \rightarrow D_s^+ \mu^+ \mu^-$  process [99]. Using the  $pp$  collision data collected by the LHCb experiment at the center-of-mass energies of 7, 8, and 13 TeV, corresponding to a total integrated luminosity of  $9 \text{ fb}^{-1}$ , the LHCb Collaboration did not observe significant signals in the non-resonant  $\mu^+ \mu^-$  modes, but set an upper limit as  $f_c/f_u \times \mathcal{B}(B_c^+ \rightarrow D_s^+ \mu^+ \mu^-) < 9.6 \times 10^{-8}$  at the 95% confidence level.

In the theoretical sector, the rare semileptonic decays of  $B_c$  have been studied by the light-front quark model (LFQM) [100], the pQCD [101], the QCD sum rule [102, 103], the constituent quark model (CQM) [100], et al. The branching fractions of  $B_c \rightarrow D_s^* \ell^+ \ell^-$  with  $\ell = e$  or  $\mu$  are predicted to be approximately  $10^{-7}$ . In this work, we also focus on the  $B_c \rightarrow D_s^* \ell^+ \ell^-$  process, where the necessary form factors are calculated via the covariant LFQM approach. To provide more physical observables, we present the angular distribution of the quasi-four-body process  $B_c \rightarrow D_s^*(\rightarrow D_s \pi) \ell^+ \ell^-$ .

The applications of the standard and(or) covariant LFQM have proved successful in the study of the meson [104–142] and baryon weak decays [143–170]. The  $B_c \rightarrow D_s^*$  weak transition form factors deduced by (axial)-vector currents have been calculated in Ref. [140] with the covariant LFQM. Probably the series of papers [110–120, 123–126, 130–139, 141, 143–166], the hadron wave function was taken as a Gaussian-like form with phenomenal parameter  $\beta$ , which represents the hadron structure. To fixed the phenomenal parameter, the corresponding decay constant was used. However, as we all know, the decay constant is only associated with the zero-point wave function. This indicates that the oversimplified Gaussian-form wave function is not able to depict the behavior far away from the zero point. For this object, we propose to directly adopt the numerical spatial wave function by solving the Schrödinger equation with the modified Godfrey-Isgur (GI) model. By fitting the mass spectrum of the observed heavy flavor mesons, the parameters of the potential model can be fixed. This strategy avoids the  $\beta$  dependence, and can also reduce the corresponding uncertainty.

This paper is organized as follows. After the Introduction, we illustrate the angular distributions of the quasi-four-body decays  $B_c \rightarrow D_s^*(\rightarrow D_s \pi) \ell^+ \ell^-$  ( $\ell = e, \mu, \tau$ ) in Sec. II. In Sec. III, we introduce the covariant LFQM and drive the formula of the weak transition form factors. And then in Sec. IV, the numerical results, including the form factors of  $B_c \rightarrow D_s^*$  and physical observables of  $B_c \rightarrow D_s^*(\rightarrow D_s \pi) \ell^+ \ell^-$  processes, are presented. Finally, this paper ends with a short summary.

## II. THE ANGULAR DISTRIBUTION OF

$$B_c \rightarrow D_s^*(\rightarrow D_s \pi) \ell^+ \ell^-$$

### A. The effective Hamiltonian for $b \rightarrow s \ell^+ \ell^-$

The effective Hamiltonian associated with  $b \rightarrow s \ell^+ \ell^-$  is [171]

$$\mathcal{H} = -\frac{4G_F}{\sqrt{2}} \left\{ V_{tb} V_{ts}^* \left[ C_1(\mu) \mathcal{O}_1^c(\mu) + C_2(\mu) \mathcal{O}_2^c(\mu) + \sum_{i=3}^{10} C_i(\mu) \mathcal{O}_i(\mu) \right] + V_{ub} V_{us}^* \left[ C_1(\mu) (\mathcal{O}_1^c(\mu) - \mathcal{O}_1^u(\mu)) + C_2(\mu) (\mathcal{O}_2^c(\mu) - \mathcal{O}_2^u(\mu)) \right] \right\}, \quad (2.1)$$

where  $V_{ij}$  are the Cabibbo-Kobayashi-Maskawa (CKM) matrix elements and  $G_F = 1.16637 \times 10^{-5} \text{ GeV}^{-2}$  [172] is the Fermi constant. Also, the  $C_i(\mu)$  are Wilson coefficients and the  $\mathcal{O}_i(\mu)$  are four fermion operators. They all depend on the QCD renormalization scale  $\mu$ . More specially, the  $\mathcal{O}_{1,2}^{c,u}$  are current-current operations, the  $\mathcal{O}_{3-6}$  are QCD penguin operators, the  $\mathcal{O}_{7,8}$  are electromagnetic and chromomagnetic penguin operators, and the  $\mathcal{O}_{9,10}$  are semileptonic operators, respectively.

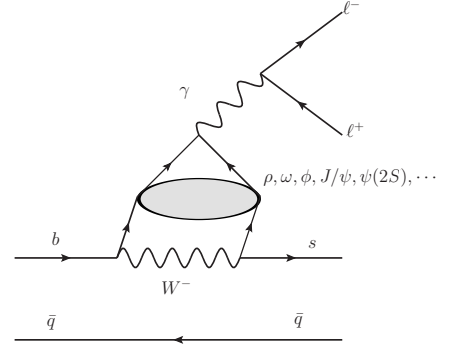


FIG. 1: The contributions of the intermediate vector states ( $\rho, \omega, \phi, J/\psi, \psi(2S), \dots$ ) to the  $b \rightarrow s \ell^+ \ell^-$  process resulting from the current-current operators  $\mathcal{O}_{1,2}^{c,u}$ .

Apart from the  $\gamma$  and  $Z$  penguin diagrams, and the  $W^+ W^-$  box diagram, the long distance contribution, via the intermediate vector states ( $\rho, \omega, \phi, J/\psi, \psi(2S), \dots$ ) (see Fig. 1) also shows an unignorable influence. By adding the factorable quark-loop contributions from  $\mathcal{O}_{1-6,8}$  to the effective Wilson coefficients  $C_{7,9}^{\text{eff}}$ , the effective Hamiltonian in Eq. (2.1) can be simplified. In the calculation, we have adopted the following effective Hamiltonian, i.e.,

$$\mathcal{H}^{\text{eff}}(b \rightarrow s \ell^+ \ell^-) = -\frac{4G_F}{\sqrt{2}} V_{tb} V_{ts}^* \frac{\alpha_e}{4\pi} \left\{ \bar{s} [C_9^{\text{eff}}(q^2, \mu) \gamma^\mu P_L - \frac{2m_b}{q^2} C_7^{\text{eff}}(\mu) i\sigma^{\mu\nu} q_\nu P_R] b (\bar{\ell} \gamma_\mu \ell) + C_{10}(\mu) (\bar{s} \gamma^\mu P_L b) (\bar{\ell} \gamma_\mu \gamma_5 \ell) \right\}, \quad (2.2)$$

where  $P_{L(R)} = (1 \mp \gamma_5)/2$ ,  $\sigma^{\mu\nu} = i(\gamma^\mu \gamma^\nu - \gamma^\nu \gamma^\mu)/2$ , and the electromagnetic coupling constant  $\alpha_e = 1/137$ . The  $C_7^{\text{eff}}$  and

$C_9^{10}$  are the effective Wilson coefficients, defined as [173]

$$\begin{aligned} C_7^{\text{eff}}(\mu) &= C_7(\mu) + C'_{b \rightarrow s\gamma}(\mu), \\ C_9^{\text{eff}}(q^2, \mu) &= C_9(\mu) + Y_{\text{pert}}(q^2, \mu) + Y_{\text{res}}(q^2, \mu), \end{aligned} \quad (2.3)$$

where the term  $C'_{b \rightarrow s\gamma}$  is the absorptive part of the  $b \rightarrow sc\bar{c} \rightarrow s\gamma$  rescattering: [47, 50, 51, 57, 66, 173–175]

$$\begin{aligned} C'_{b \rightarrow s\gamma}(\mu) &= i\alpha_s \left\{ \frac{2}{9} \eta^{\frac{14}{23}} \left[ \frac{x_t(x_t^2 - 5x_t - 2)}{8(x_t - 1)^3} + \frac{3x_t^2 \ln x_t}{4(x_t - 1)^4} - 0.1687 \right] \right. \\ &\quad \left. - 0.03C_2(\mu) \right\} \end{aligned} \quad (2.4)$$

with  $x_t = m_t^2/m_W^2$ ,  $\eta = \alpha_s(m_W)/\alpha_s(\mu)$ , and  $\alpha_s$  being adopted as  $\alpha_s(m_b) = 0.217$  in our calculation. The short-distance contributions from the soft-gluon emission and the one-loop contributions of the four fermion operators  $O_1 - O_6$ , and the long-distance contributions from the intermediate vector meson states are also taken into account, and have been included in the  $Y_{\text{pert}}$  and  $Y_{\text{res}}$  terms, respectively. The  $Y_{\text{pert}}$  can be written as [176]

$$\begin{aligned} Y_{\text{pert}}(\hat{s}, \mu) &= 0.124\omega(\hat{s}) + g(\hat{m}_c, \hat{s})C(\mu) \\ &\quad + \lambda_u \left[ g(\hat{m}_c, \hat{s}) - g(0, \hat{s}) \right] (3C_1(\mu) + C_2(\mu)) \\ &\quad - \frac{1}{2}g(0, \hat{s})(C_3(\mu) + 3C_4(\mu)) \\ &\quad - \frac{1}{2}g(1, \hat{s})(4C_3(\mu) + 4C_4(\mu) + 3C_5(\mu) + C_6(\mu)) \\ &\quad + \frac{2}{9}(3C_3(\mu) + C_4(\mu) + 3C_5(\mu) + C_6(\mu)), \end{aligned} \quad (2.5)$$

where  $\hat{s} = q^2/m_b^2$  and  $\hat{m}_c = m_c/m_b$  with  $m_b = 4.8$  GeV and  $m_c = 1.6$  GeV, and  $C(\mu) = 3C_1(\mu) + C_2(\mu) + 3C_3(\mu) + C_4(\mu) + 3C_5(\mu) + C_6(\mu)$ . At the next leading order, the Wilson coefficients at the QCD renormalization scale  $\mu = m_b$  are chosen as  $C_1 = -0.175$ ,  $C_2 = 1.076$ ,  $C_3 = 1.258\%$ ,  $C_4 = -3.279\%$ ,  $C_5 = 1.112\%$ ,  $C_6 = -3.634\%$ ,  $C_7 = -0.302$ ,  $C_8 = -0.148$ ,  $C_9 = 4.232$ , and  $C_{10} = -4.410$  [171].

In the Wolfenstein representation, the  $\lambda_u = V_{ub}V_{us}^*/(V_{tb}V_{ts}^*)$  can be expressed as

$$\lambda_u \approx -\lambda^2(\rho - i\eta), \quad (2.6)$$

approximately, which is a small value suppressed by  $\lambda^2$  with  $\lambda = 0.22500 \pm 0.00067$  [172].

In addition, the term  $\Omega(\hat{s})$  is the one-gluon correction to the matrix element of the operator  $O_9$ , represented as [50, 176]

$$\begin{aligned} \omega(\hat{s}) &= -\frac{2}{9}\pi^2 + \frac{4}{3} \int_0^{\hat{s}} \frac{\ln 1-u}{u} du - \frac{2}{3} \ln(\hat{s}) \ln(1-\hat{s}) \\ &\quad - \frac{5+4\hat{s}}{3(1+2\hat{s})} \ln(1-\hat{s}) - \frac{2\hat{s}(1+\hat{s})(1-2\hat{s})}{3(1-\hat{s})^2(1+2\hat{s})} \ln(\hat{s}) \\ &\quad + \frac{5+9\hat{s}-6\hat{s}^2}{6(1-\hat{s})(1+2\hat{s})}, \end{aligned} \quad (2.7)$$

and the  $g$  terms: [47, 57, 66, 174, 176]

$$\begin{aligned} g(z, \hat{s}) &= -\frac{8}{9} \ln z + \frac{8}{27} + \frac{4}{9}x - \frac{2}{9}(2+x)\sqrt{|1-x|} \\ &\quad \times \begin{cases} \ln \left| \frac{1+\sqrt{1-x}}{1-\sqrt{1-x}} \right| - i\pi & \text{for } x \equiv 4z^2/\hat{s} < 1 \\ 2 \arctan \frac{1}{\sqrt{x-1}} & \text{for } x \equiv 4z^2/\hat{s} > 1 \end{cases}, \\ g(0, \hat{s}) &= \frac{8}{27} - \frac{8}{9} \ln \frac{m_b}{\mu} - \frac{4}{9} \ln \hat{s} + \frac{4}{9}i\pi, \end{aligned} \quad (2.8)$$

come from the one-loop contributions of the  $O_{1-6}$ .

The  $Y_{\text{res}}$  term, which describes the long-distance contributions associated with the intermediate light vector mesons (such as  $\rho$ ,  $\omega$ , and  $\phi$ ) and vector charmonium states (such as  $J/\psi$ ,  $\psi(2S)$ , etc.) (see the Fig. 1), is adopted as [50]<sup>1</sup>

$$\begin{aligned} Y_{\text{res}}(q^2, \mu) &= -\frac{3\pi}{\alpha_e^2} \left[ C(\mu) \sum_{V_i=J/\psi, \psi(2S), \dots} \frac{m_{V_i} \mathcal{B}(V_i \rightarrow \ell^+ \ell^-) \Gamma_{V_i}}{q^2 - m_{V_i}^2 + im_{V_i} \Gamma_{V_i}} \right. \\ &\quad \left. - \lambda_u g(0, \hat{s}) (3C_1(\mu) + C_2(\mu)) \right. \\ &\quad \left. \times \sum_{V_j=\rho, \omega, \phi} \frac{m_{V_j} \mathcal{B}(V_j \rightarrow \ell^+ \ell^-) \Gamma_{V_j}}{q^2 - m_{V_j}^2 + im_{V_j} \Gamma_{V_j}} \right], \end{aligned} \quad (2.9)$$

where  $m_{V_i}$  and  $\Gamma_{V_i}$  are the mass and total width of the intermediate vector meson  $V_i$  respectively, and the  $\Gamma(V_i \rightarrow \ell^+ \ell^-)$  is the corresponding dilepton width. These input values are collected in Table I. In addition, the non-vanished branching fraction for the  $\tau$  channel, i.e.,  $\mathcal{B}(\psi(2S) \rightarrow \tau^+ \tau^-) = 3.1 \times 10^{-3}$  [172], is also used.

For the  $J/\psi$  and  $\psi(2S)$  states, the small widths and the large dilepton width will have large influence on the decay width. However, the narrow widths are also used to reject them in the experimental analysis. On the other hand, for those above the  $D\bar{D}$  threshold, such as  $\psi(3770)$ ,  $\psi(4040)$  and  $\psi(4160)$ , the board widths and mutual overlap make thing difficult. Also, for the charmless vector mesons ( $\rho$ ,  $\omega$  and  $\phi$ ), their contributions are suppressed by the  $\lambda_u$  factor.

TABLE I: The masses, total widths and dilepton widths of the intermediate vector mesons used in Eq. (2.9). These values are quoted from the PDG [172].

$V_i$	$m_{V_i}$ (GeV)	$\Gamma_{V_i}$ (MeV)	$\mathcal{B}(V_i \rightarrow \ell^+ \ell^-)$ where $\ell = e, \mu$
$\rho$	0.775	149	$4.635 \times 10^{-5}$
$\omega$	0.783	8.68	$7.380 \times 10^{-5}$
$\phi$	1.019	4.249	$2.915 \times 10^{-4}$
$J/\psi$	3.097	0.093	$5.966 \times 10^{-2}$
$\psi(2S)$	3.686	0.294	$7.965 \times 10^{-3}$
$\psi(3770)$	3.774	27.2	$9.6 \times 10^{-6}$
$\psi(4040)$	4.039	80	$1.07 \times 10^{-5}$
$\psi(4160)$	4.191	70	$6.9 \times 10^{-6}$

<sup>1</sup> This is a phenomenological method, and for more details on the charm-loop contribution, one can refer to Refs. [177, 178].

### B. The angular distributions and physical observables in the $B_c \rightarrow D_s^*(\rightarrow D_s \pi) \ell^+ \ell^-$ decay

With the effective Hamiltonian in Eq. (2.2), we can calculate the quasi-four-body decay  $B_c^- \rightarrow D_s^{*-}(\rightarrow D_s^- \pi^0) \ell^+ \ell^-$ . As deduced in Ref. [179], the corresponding angular distributions can be simplified as

$$\frac{d^4\Gamma}{dq^2 d\cos\theta d\cos\theta_\ell d\phi} = \frac{9}{32\pi} \sum_i I_i(q^2) f_i(\theta, \theta_\ell, \phi), \quad (2.10)$$

where the explicit expressions of  $I_i(q^2)$  and  $f_i(\theta, \theta_\ell, \phi)$  are shown in Table II. Compared to Ref. [179], the term  $nI_{6c}$  is

neglected since it depends on the scalar operator. The  $\theta$  is the angle between the  $+\hat{z}$  direction and pion-emitted direction in the rest frame of the  $D_s^*$  meson, the  $\theta_\ell$  is the angle made by the  $\ell^-$  with the  $+\hat{z}$  direction in the  $\ell^+ \ell^-$  center of mass system, and the  $\phi$  is the angle between the decay planes, i.e., the  $D_s^* \rightarrow D_s \pi$  plane and the virtual boson  $\rightarrow \ell^+ \ell^-$  plane.

The amplitudes  $\mathcal{A}_{0,\parallel,\perp}^{L,R}$  and  $\mathcal{A}_t$  are the functions of the transferred momentum square  $q^2$ , and the seven independent form factors  $V$ ,  $A_{0,1,2}$  and  $T_{1,2,3}$ , i.e., [50, 51, 179]

$$\begin{aligned} \mathcal{A}_\perp^{L,R}(q^2) &= -N_\ell \sqrt{2N_{D_s^*}} \sqrt{\lambda(M'^2, M''^2, q^2)} \left[ (C_9^{\text{eff}} \mp C_{10}) \frac{V(q^2)}{M' + M''} + 2\hat{m}_b C_7^{\text{eff}} T_1(q^2) \right], \\ \mathcal{A}_\parallel^{L,R}(q^2) &= N_\ell \sqrt{2N_{D_s^*}} \left[ (C_9^{\text{eff}} \mp C_{10}) (M' + M'') A_1(q^2) + 2\hat{m}_b C_7^{\text{eff}} (M'^2 - M''^2) T_2(q^2) \right], \\ \mathcal{A}_0^{L,R}(q^2) &= \frac{N_\ell \sqrt{N_{D_s^*}}}{2M'' \sqrt{q^2}} \left\{ (C_9^{\text{eff}} \mp C_{10}) \left[ (M'^2 - M''^2 - q^2) (M' + M'') A_1(q^2) - \frac{\lambda(M'^2, M''^2, q^2)}{M' + M''} A_2(q^2) \right] \right. \\ &\quad \left. + 2\hat{m}_b C_7^{\text{eff}} \left[ (M'^2 + 3M''^2 - q^2) T_2(q^2) - \frac{\lambda(M'^2, M''^2, q^2)}{M'^2 - M''^2} T_3(q^2) \right] \right\}, \\ \mathcal{A}_t(q^2) &= 2N_\ell \sqrt{N_{D_s^*}} \sqrt{\frac{\lambda(M'^2, M''^2, q^2)}{q^2}} C_{10} A_0(q^2), \end{aligned} \quad (2.11)$$

where  $\lambda(x, y, z) = x^2 + y^2 + z^2 - 2(xy + xz + yz)$  and  $\hat{m}_b = m_b/q^2$ , and

$$\begin{aligned} N_\ell &= \frac{i\alpha_e G_F}{4\sqrt{2}\pi} V_{ib} V_{ts}^*, \\ N_{D_s^*} &= \frac{8\sqrt{\lambda} q^2}{3 \times 256\pi^3 M'^3} \sqrt{1 - \frac{4m_\ell^2}{q^2}} \mathcal{B}(D_s^* \rightarrow D_s \pi). \end{aligned} \quad (2.12)$$

For the  $CP$ -conjugated mode  $B_c^+ \rightarrow D_s^{*+}(\rightarrow D_s^+ \pi^0) \ell^+ \ell^-$ , we have

$$\frac{d^4\bar{\Gamma}}{dq^2 d\cos\theta d\cos\theta_\ell d\phi} = \sum_i \frac{9}{32\pi} \bar{I}_i(q^2) f_i(\theta, \theta_\ell, \phi), \quad (2.13)$$

where  $\bar{I}_i$  can be obtained by doing the conjugation for the weak phases of the CKM matrix elements in  $I_i$  in Table II. In addition, we should also do the following substitutions as:

$$\begin{aligned} I_{1(c,s),2(c,s),3,4,7} &\rightarrow \bar{I}_{1(c,s),2(c,s),3,4,7}, \\ I_{5,6s,8,9} &\rightarrow -\bar{I}_{5,6s,8,9}. \end{aligned} \quad (2.14)$$

This is the result of the operations of  $\theta_\ell \rightarrow \theta_\ell - \pi$  and  $\phi \rightarrow -\phi$ .

To separate the  $CP$ -conserving and the  $CP$ -violating effects, we define the normalized  $CP$ -averaged angular coefficients

$S_i$  and the  $CP$  asymmetry angular coefficients  $A_i$  as

$$\begin{aligned} S_i &= \frac{I_i + \bar{I}_i}{d(\Gamma + \bar{\Gamma})/dq^2}, \\ A_i &= \frac{I_i - \bar{I}_i}{d(\Gamma + \bar{\Gamma})/dq^2}, \end{aligned} \quad (2.15)$$

respectively. To reduce both the experimental and theoretical uncertainties, the  $S_i$  and  $A_i$  have been normalized to the  $CP$ -averaged differential decay width. The other physical observables, such as the forward-backward asymmetry parameter  $A_{FB}$ , the  $CP$ -violation  $\mathcal{A}_{CP}$ , and the longitudinal (transverse) polarization fractions of  $D_s^*$  meson  $F_L(F_T)$ , can thus be easily expressed in terms of these normalized angular coefficients. With the above preparations, we continue to study the physical observables, i.e.,

- (a) By integrating over the angles in the regions  $\theta \in [0, \pi]$ ,  $\theta_\ell \in [0, \pi]$ , and  $\phi \in [0, 2\pi]$ , the  $q^2$ -dependent differential decay width becomes

$$\frac{d\Gamma}{dq^2} = \frac{1}{4} (3I_{1c} + 6I_{1s} - I_{2c} - 2I_{2s}), \quad (2.16)$$

and that of the  $CP$ -conjugated mode  $d\bar{\Gamma}/dq^2$  is analogous and can be obtained with the replacement in

TABLE II: The explicit expressions of the angular coefficients  $I_i$  and  $f_i$  [50, 51, 179] in Eq. (2.10), where  $\hat{m}_\ell^2 = m_\ell^2/q^2$  and  $\beta_\ell = \sqrt{1 - 4\hat{m}_\ell^2}$ .

$i$	$I_i(q^2)$	$f_i(\theta, \theta_\ell, \phi)$
1s	$(\frac{3}{4} - \hat{m}_\ell^2)( \mathcal{A}_\parallel^L ^2 +  \mathcal{A}_\perp^L ^2 +  \mathcal{A}_\parallel^R ^2 +  \mathcal{A}_\perp^R ^2) + 4\hat{m}_\ell^2 \text{Re}[\mathcal{A}_\perp^L \mathcal{A}_\perp^{R*} + \mathcal{A}_\parallel^L \mathcal{A}_\parallel^{R*}]$	$\sin^2 \theta$
1c	$ \mathcal{A}_0^L ^2 +  \mathcal{A}_0^R ^2 + 4\hat{m}_\ell^2( \mathcal{A}_\parallel^L ^2 + 2\text{Re}[\mathcal{A}_0^L \mathcal{A}_0^{R*}])$	$\cos^2 \theta$
2s	$\beta_\ell^2( \mathcal{A}_\parallel^L ^2 +  \mathcal{A}_\perp^L ^2 +  \mathcal{A}_\parallel^R ^2 +  \mathcal{A}_\perp^R ^2)/4$	$\sin^2 \theta \cos 2\theta_\ell$
2c	$-\beta_\ell^2( \mathcal{A}_0^L ^2 +  \mathcal{A}_0^R ^2)$	$\cos^2 \theta \cos 2\theta_\ell$
3	$\beta_\ell^2( \mathcal{A}_\perp^L ^2 -  \mathcal{A}_\parallel^L ^2 +  \mathcal{A}_\perp^R ^2 -  \mathcal{A}_\parallel^R ^2)/2$	$\sin^2 \theta \sin^2 \theta_\ell \cos 2\phi$
4	$\beta_\ell^2 \text{Re}[\mathcal{A}_0^L \mathcal{A}_\parallel^{L*} + \mathcal{A}_0^R \mathcal{A}_\parallel^{R*}]/\sqrt{2}$	$\sin 2\theta \sin 2\theta_\ell \cos \phi$
5	$\sqrt{2}\beta_\ell \text{Re}[\mathcal{A}_0^L \mathcal{A}_\perp^{L*} - \mathcal{A}_0^R \mathcal{A}_\perp^{R*}]$	$\sin 2\theta \sin \theta_\ell \cos \phi$
6s	$2\beta_\ell \text{Re}[\mathcal{A}_\parallel^L \mathcal{A}_\perp^{L*} - \mathcal{A}_\parallel^R \mathcal{A}_\perp^{R*}]$	$\sin^2 \theta \cos \theta_\ell$
7	$\sqrt{2}\beta_\ell \text{Im}[\mathcal{A}_0^L \mathcal{A}_\parallel^{L*} - \mathcal{A}_0^R \mathcal{A}_\parallel^{R*}]$	$\sin 2\theta \sin \theta_\ell \sin \phi$
8	$\beta_\ell^2 \text{Im}[\mathcal{A}_0^L \mathcal{A}_\perp^{L*} + \mathcal{A}_0^R \mathcal{A}_\perp^{R*}]/\sqrt{2}$	$\sin 2\theta \sin 2\theta_\ell \sin \phi$
9	$\beta_\ell^2 \text{Im}[\mathcal{A}_\parallel^L \mathcal{A}_\perp^{L*} + \mathcal{A}_\parallel^R \mathcal{A}_\perp^{R*}]$	$\sin^2 \theta \sin^2 \theta_\ell \sin 2\phi$

Eq. (2.14). So the  $CP$ -averaged differential decay width of  $B_c \rightarrow D_s^*(\rightarrow D_s \pi) \ell^+ \ell^-$  can be evaluated by

$$\frac{d\Gamma}{dq^2} = \frac{1}{2} \left( \frac{d\Gamma}{dq^2} + \frac{d\bar{\Gamma}}{dq^2} \right). \quad (2.17)$$

In this work, we focus on the  $CP$ -averaged decay width.

(b) The  $CP$  violation of the decay width can thus be estimated by

$$\mathcal{A}_{CP}(q^2) = \frac{(d\Gamma - d\bar{\Gamma})/dq^2}{(d\Gamma + d\bar{\Gamma})/dq^2} = \frac{1}{4}(3A_{1c} + 6A_{1s} - A_{2c} - 2A_{2s}). \quad (2.18)$$

(c) The  $CP$  asymmetry lepton forward-backward asymmetry is

$$A_{FB}^{CP}(q^2) = \frac{(\int_{-1}^0 - \int_0^1) d\cos\theta_\ell \int_{-1}^1 d\cos\theta \int_0^{2\pi} d\phi \frac{d^4(\Gamma + \bar{\Gamma})}{dq^2 d\cos\theta d\cos\theta_\ell d\phi}}{d(\Gamma + \bar{\Gamma})/dq^2} = \frac{3}{4}A_6, \quad (2.19)$$

and the  $CP$ -averaged lepton forward-backward asymmetry is

$$A_{FB}(q^2) = \frac{3}{4}S_6. \quad (2.20)$$

(d) The longitudinal and transverse  $D_s^*$  polarization fractions are

$$\begin{aligned} F_L &= \frac{1}{4}(3S_{1c} - S_{2c}), \\ F_T &= \frac{1}{2}(3S_{1s} - S_{2s}), \end{aligned} \quad (2.21)$$

respectively.

Furthermore, the clean angular observables  $P_{1,2,3}$  and  $P'_{4,5,6,8}$  are associated with the  $CP$ -averaged angular coefficients:

$$\begin{aligned} P_1 &= \frac{S_3}{2S_{2s}}, \\ P_2 &= \frac{\beta_\ell S_{6s}}{8S_{2s}}, \\ P_3 &= -\frac{S_9}{4S_{2s}}, \end{aligned} \quad (2.22)$$

$$\begin{aligned} P'_4 &= \frac{S_4}{\sqrt{S_{1c}S_{2s}}}, \\ P'_5 &= \frac{\beta_\ell S_5}{2\sqrt{S_{1c}S_{2s}}}, \\ P'_6 &= -\frac{\beta_\ell S_7}{2\sqrt{S_{1c}S_{2s}}}, \\ P'_8 &= -\frac{S_8}{\sqrt{S_{1c}S_{2s}}}. \end{aligned} \quad (2.23)$$

In the large-recoiled limit, these observables are largely free of form factor uncertainties.

Finally, we also focus on the ratios, i.e.,

$$\begin{aligned} R^{e\mu} &= \frac{\int_{4m_\mu^2}^{(M'-M'')^2} \frac{d\Gamma[B_c \rightarrow D_s^*(\rightarrow D_s \pi) e^+ e^-] dq^2}{\int_{4m_\mu^2}^{(M'-M'')^2} \frac{d\Gamma[B_c \rightarrow D_s^*(\rightarrow D_s \pi) \mu^+ \mu^-] dq^2}, \\ R^{\tau\mu} &= \frac{\int_{4m_\mu^2}^{(M'-M'')^2} \frac{d\Gamma[B_c \rightarrow D_s^*(\rightarrow D_s \pi) \tau^+ \tau^-] dq^2}{\int_{4m_\mu^2}^{(M'-M'')^2} \frac{d\Gamma[B_c \rightarrow D_s^*(\rightarrow D_s \pi) \mu^+ \mu^-] dq^2}, \end{aligned} \quad (2.24)$$

which reflect the LFU. We would like to emphasize that the lower limit of the integral of the electron mode are chosen as  $4m_\mu^2$  instead of the kinematic limit  $4m_e^2$  in order to exclude the large enhancement dominated by the photon pole in small  $q^2$  region due to the  $C_7^{\text{eff}}$ -associated factor  $1/q^2$ . In the  $B \rightarrow K\ell^+\ell^-$  process, the experimental measurements of the ratio



$R_K^{e\mu}$  by Belle [8–11] and *BABAR* [14] are in agreement with the SM prediction, while the LHCb result [18, 20, 21] shows a clear deviation from the SM expectation (see the Fig. 4 of Ref. [21]) with  $3.1\sigma$ . The ratio in the  $B_c \rightarrow D_s^* \ell^+ \ell^-$  sector is also interesting to investigate whether it is consistent with the SM expectation or not. The breaking of the LFU requires an expansion of the gauge structure of the SM, and of course probes the NP effects [180].

### III. WEAK TRANSITION FORM FACTORS

The standard and(or) covariant LFQM have been widely used to study the decays of mesons [104–142] and baryons [143–170]. In the conventional LFQM framework, the consistent quark (or anti-quark) of the meson is required to be on its mass shell, and thus the initial (or final) meson

is off-shell. This procedure misses the zero-mode effects and makes the matrix element non-covariant. To avoid this shortcoming, W. Jaus [104, 108] proposed a covariant framework for the  $S$ -waved pseudoscalar and vector meson decays in which the zero-mode contributions are systematically taken into account. Cheng et al, [110, 118] extended this approach to case of  $P$ -wave meson (such as scalar, axial-vector and tensor mesons). The physical quantities, such as the decay constant and the form factor of the weak transition, are obtained in terms of the Feynman loop integration. Unlike the conventional LFQM, the covariant LFQM requires the initial (or final) meson to be on its mass shell. For more details on the difference, see Refs. [110, 132]. In this section, we will use the covariant LFQM to calculate the  $B_c \rightarrow D_s^*$  form factors.

Following the Ref. [140], the  $B_c \rightarrow D_s^*$  weak transition form factors deduced by (axial-)vector currents are defined as

$$\begin{aligned} \langle D_s^*(p'') | \bar{s} \gamma_\mu b | B_c(p') \rangle &= \epsilon_{\mu\nu\alpha\beta} \varepsilon^{*\nu} P^\alpha q^\beta g(q^2), \\ \langle D_s^*(p'') | \bar{s} \gamma_\mu \gamma_5 b | B_c(p') \rangle &= -i \left\{ \varepsilon_\mu^* f(q^2) + \varepsilon^* \cdot P (P_\mu a_+(q^2) + q_\mu a_-(q^2)) \right\}, \end{aligned} \quad (3.1)$$

where we use the convention  $\epsilon_{0123} = +1$  and define  $P_\mu = p'_\mu + p''_\mu$  and  $q_\mu = p'_\mu - p''_\mu$ , and  $\varepsilon$  is the polarization vector of the  $D_s^*$  meson. These amplitudes can also be parameterized as the Bauer-Stech-Wirbel (BSW) form [181], i.e.,

$$\begin{aligned} \langle D_s^*(p'') | \bar{s} \gamma_\mu b | B_c(p') \rangle &= -\frac{1}{M' + M''} \epsilon_{\mu\nu\alpha\beta} \varepsilon^{*\nu} P^\alpha q^\beta V(q^2), \\ \langle D_s^*(p'') | \bar{s} \gamma_\mu \gamma_5 b | B_c(p') \rangle &= i \left\{ (M' + M'') \varepsilon_\mu^* A_1(q^2) - \frac{\varepsilon^* \cdot P}{M' + M''} P_\mu A_2(q^2) - 2M'' \frac{\varepsilon^* \cdot P}{q^2} q_\mu [A_3(q^2) - A_0(q^2)] \right\} \end{aligned} \quad (3.2)$$

with  $M'$  ( $M''$ ) being the mass of the parent (daughter) meson. These two definitions are related by the relations [140]:

$$\begin{aligned} V(q^2) &= -(M' + M'') g(q^2), \quad A_1(q^2) = -\frac{f(q^2)}{M' + M''}, \\ A_2(q^2) &= (M' + M'') a_+(q^2), \quad A_3(q^2) - A_0(q^2) = \frac{q^2}{2M''} a_-(q^2), \\ A_3(q^2) &= \frac{M' + M''}{2M''} A_1(q^2) - \frac{M' - M''}{2M''} A_2(q^2). \end{aligned} \quad (3.3)$$

In addition, the (pseudo-)tensor current amplitudes can be defined as [182, 183]

$$\begin{aligned} \langle D_s^*(p'') | \bar{s} i \sigma_{\mu\nu} q^\nu b | B_c(p') \rangle &= T_1(q^2) \epsilon_{\mu\nu\alpha\beta} \varepsilon^{*\nu} P^\alpha q^\beta, \\ \langle D_s^*(p'') | \bar{s} i \sigma_{\mu\nu} q^\nu \gamma_5 b | B_c(p') \rangle &= iT_2(q^2) \left[ (M'^2 - M''^2) \varepsilon_\mu^* - \varepsilon^* \cdot q P_\mu \right] + iT_3(q^2) \varepsilon^* \cdot q \left[ q_\mu - \frac{q^2}{M'^2 - M''^2} P_\mu \right], \end{aligned} \quad (3.4)$$

where, we have  $T_1(0) = T_2(0)$  since the identity  $2\sigma_{\mu\nu}\gamma_5 = -i\epsilon_{\mu\nu\alpha\beta}\sigma^{\alpha\beta}$ .

The form factors require a non-perturbative calculation. In this work, we use the covariant LFQM to calculate the relevant form factors for the weak transition. In this approach, the constituent quark and the antiquark inside a meson are off-shell. We define the incoming (outgoing) meson to have the momentum  $P' = p'_1 + p_2$  ( $P'' = p''_1 + p_2$ ), where  $p_1^{(\prime\prime)}$  and  $p_2$

are the off-shell momenta of the quark and the antiquark, respectively. These momenta can be expressed in terms of the internal variables  $(x_i, \vec{k}_\perp)$  ( $i = 1, 2$ ), defined by

$$p_1^{+\prime} = x_1 P^{+\prime}, \quad p_1^{+\prime} = x_2 P^{+\prime}, \quad \vec{p}_{1\perp}^{\prime} = x_1 \vec{P}_{\perp}^{\prime} + \vec{k}_{\perp}^{\prime}. \quad (3.5)$$

They must also satisfy  $x_1 + x_2 = 1$ .

According to Refs. [110, 140], the corresponding weak transition matrix element at the one-loop level can be calcu-

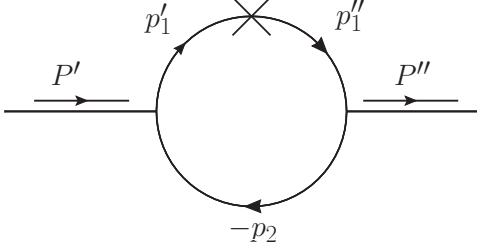


FIG. 2: The one-loop Feynman diagram for meson weak transition amplitude, where  $P'$  ( $P''$ ) is the momentum of the incoming (outgoing) meson,  $p_1^{(\prime\prime)}$  and  $p_2$  are the momenta of the quark and antiquark, respectively. The  $X$  denotes the weak interaction vertex.

lated in terms of the Feynman loop integral, as shown as in Fig. 2. And then the form factors can be extracted from the corresponding matrix element. To write down the transition amplitude, we need the meson-quark antiquark vertices for the initial meson as  $i\Gamma' = H'_P\gamma_5$ , and that of the outgoing meson as  $i(\gamma_0\Gamma''^\dagger\gamma_0)$  with  $\Gamma'' = H''_V[\gamma_\mu - (p_1'' - p_2)_\mu/W_V'']$  [110, 140], where the subscripts  $P$  and  $V$  denote the pseudo-scalar and vector meson, respectively.

For Fig. 2, the concrete expression of the transition amplitude for  $P \rightarrow V$  can be expressed as

$$\mathcal{B}_\mu^{V(A,T,T5)} = -i^3 \frac{N_c}{(2\pi)^4} \int d^4 p_1' \frac{iH'_P H''_V}{N_1' N_1'' N_2} S_{\mu\nu}^{V(A,T,T5)} \epsilon_{\nu}^{*\nu}, \quad (3.6)$$

where  $N_1^{(\prime\prime)} = p_1^{(\prime\prime)2} - m_1^{(\prime\prime)2}$  and  $N_2 = p_2^2 - m_2^2$  come from the propagators of the quarks. The superscripts  $V$ ,  $A$ ,  $T$ , and  $T5$  represent the vector, axial-vector, tensor, and pseudo-tensor currents, respectively. The traces  $S_{\mu\nu}^V$  are written as

$$\begin{aligned} S_{\mu\nu}^V &= \text{Tr} \left[ \left( \gamma_\nu - \frac{(p_1'' - p_2)_\nu}{W_V''} \right) (\not{p}_1'' + m_1'') \gamma_\mu (\not{p}_1' + m_1') \gamma_5 (-\not{p}_2 + m_2) \right] \\ &= -2i\epsilon_{\mu\alpha\beta} \left[ p_1'^\alpha P^\beta (m_1'' - m_1') + p_1'^\alpha q^\beta (m_1'' + m_1' - 2m_2) \right. \\ &\quad \left. + q^\alpha P^\beta m_1' \right] + \frac{1}{W_V''} (4p_{1\nu}' - 3q_\nu - P_\nu) i\epsilon_{\mu\alpha\beta\rho} p_1'^\alpha q^\beta P^\rho. \end{aligned} \quad (3.7)$$

To make reading easier, the relevant expressions of the traces  $S_{\mu\nu}^{A,T,T5}$  are collected in Appendix A.

Following the Refs. [109, 110, 118], the execution of the  $p_1'$  integration went to the replacement:

$$\begin{aligned} N_1^{(\prime\prime)} &\rightarrow \hat{N}_1^{(\prime\prime)} = x_1(M'^{(\prime\prime)2} - M_0'^{(\prime\prime)2}), \\ H_{P(V)}^{(\prime\prime)} &\rightarrow h_{P(V)}^{(\prime\prime)}, \\ W_V'' &\rightarrow \omega_V'', \end{aligned} \quad (3.8)$$

$$\int \frac{d^4 p_1'}{(2\pi)^4} H'_P H''_V S_{\mu\nu} \epsilon^{*\nu} \rightarrow -i\pi \int \frac{dx_2 d^2 \vec{k}_\perp}{x_2 \hat{N}_1' \hat{N}_1''} h'_P h_V'' \hat{S}_{\mu\nu} \epsilon^{*\nu},$$

where we define

$$M_0'^{(\prime\prime)2} = \frac{\vec{k}_\perp'^{(\prime\prime)2} + m_1'^{(\prime\prime)2}}{x_1} + \frac{\vec{k}_\perp'^{(\prime\prime)2} + m_2'^{(\prime\prime)2}}{x_2}, \quad (3.9)$$

with  $\vec{k}_\perp'' = \vec{k}_\perp' - x_2 \vec{q}_\perp$  and  $\omega_V'' = M_0'' + m_1'' + m_2$ .

To write down the concrete expression of  $\hat{S}_{\mu\nu}$ , we should take into account the so-called zero-mode contribution. As shown in Refs. [110, 127], after doing the integration in Eq. (3.8) we have  $p_2 = \hat{p}_2$ , and

$$\begin{aligned} \hat{p}_1^\mu &= (P' - \hat{p}_2)^\mu \\ &= x_1 P^\mu + (0, 0, \vec{k}_\perp')^\mu + \frac{1}{2} \left( x_2 P'^- - \frac{\vec{p}_{2\perp}^2 + m_2^2}{x_2 P'^+} \right) \tilde{\omega}^\mu, \end{aligned} \quad (3.10)$$

where  $\tilde{\omega} = (2, 0, \vec{0}_\perp)$  is a light-like four vector in the light-front coordinate. Following the discussions in a series papers [109, 110, 118, 127], for avoiding the  $\tilde{\omega}$  dependence, we need to do the following replacements [109, 110, 118]

$$\begin{aligned} \hat{p}_{1\mu}' &\doteq P_\mu A_1^{(1)} + q_\mu A_2^{(1)}, \\ \hat{p}_{1\mu}' \hat{p}_{1\nu}' &\doteq g_{\mu\nu} A_1^{(2)} + P_\mu P_\nu A_2^{(2)} + (P_\mu q_\nu + P_\nu q_\mu) A_3^{(2)} + q_\mu q_\nu A_4^{(2)}, \\ N_2 &\doteq Z_2, \\ \hat{p}_{1\mu}' \hat{N}_2 &\doteq q_\mu \left( A_2^{(1)} Z_2 + \frac{P \cdot q}{q^2} A_1^{(2)} \right), \\ \hat{p}_{1\mu}' \hat{p}_{1\nu}' \hat{N}_2 &\doteq g_{\mu\nu} A_1^{(2)} Z_2 + q_\mu q_\nu \left[ A_4^{(2)} Z_2 + 2 \frac{P \cdot q}{q^2} A_2^{(1)} A_1^{(2)} \right], \end{aligned} \quad (3.11)$$

in Eq. (3.7), Eq. (A.1), Eq. (A.4), and Eq. (A.5). Here,  $Z_2 = \hat{N}_1' + m_1'^2 - m_2^2 + (1 - 2x_1)M'^2 + (q^2 + P \cdot q) \frac{\vec{k}_\perp' \cdot \vec{q}_\perp}{q^2}$ ,  $P \cdot q = M'^2 - M''^2$ , and

$$\begin{aligned} A_1^{(1)} &= \frac{x_1}{2}, \quad A_2^{(1)} = A_1^{(1)} - \frac{\vec{k}_\perp' \cdot \vec{q}_\perp}{q^2}, \\ A_1^{(2)} &= -\vec{k}_\perp'^2 - \frac{(\vec{k}_\perp' \cdot \vec{q}_\perp)^2}{q^2}, \quad A_2^{(2)} = (A_1^{(1)})^2, \\ A_3^{(2)} &= A_1^{(1)} A_2^{(1)}, \quad A_4^{(2)} = (A_2^{(1)})^2 - \frac{1}{q^2} A_1^{(2)}. \end{aligned} \quad (3.12)$$

After performing the replacements (3.11) in the decay amplitudes (3.7) and (A.1), the form factors  $g$ ,  $f$ ,  $a_+$ , and  $a_-$  can be obtained from the terms who are proportional to the  $\epsilon_{\mu\alpha\beta} P^\alpha q^\beta$ ,  $g_{\mu\nu}$ ,  $P_\mu P_\nu$  and  $P_\mu q_\nu$ , and  $q_\mu P_\nu$  and  $q_\mu q_\nu$ , respectively. The  $\epsilon_V^{*\mu} P_\mu'' = 0$  is used here. Finally, the expressions of these form factors in covariant LFQM can be written as [108, 110, 140]

$$g(q^2) = -\frac{N_c}{16\pi^3} \int dx_2 d^2 \vec{k}_\perp \frac{2h'_P h''_V}{x_2 \hat{N}'_1 \hat{N}''_1} \left\{ x_2 m'_1 + x_1 m_2 + (m'_1 - m''_1) \frac{k'_\perp \cdot q_\perp}{q^2} + \frac{2}{\omega''_V} \left[ k_\perp'^2 + \frac{(k'_\perp \cdot q_\perp)^2}{q^2} \right] \right\}, \quad (3.13)$$

$$\begin{aligned} f(q^2) = & \frac{N_c}{16\pi^3} \int dx_2 d^2 \vec{k}_\perp \frac{h'_P h''_V}{x_2 \hat{N}'_1 \hat{N}''_1} \left\{ 2x_1(m_2 - m'_1)(M_0'^2 + M_0''^2) - 4x_1 m''_1 M_0'^2 + 2x_2 m'_1 P \cdot q + 2m_2 q^2 \right. \\ & - 2x_1 m_2 (M'^2 + M''^2) + 2(m'_1 - m_2)(m'_1 + m''_1)^2 + 8(m'_1 - m_2) \left[ k_\perp'^2 + \frac{(k'_\perp \cdot q_\perp)^2}{q^2} \right] \\ & + 2(m'_1 + m''_1)(q^2 + P \cdot q) \frac{k'_\perp \cdot q_\perp}{q^2} - 4 \frac{q^2 k_\perp'^2 + (k'_\perp \cdot q_\perp)^2}{q^2 \omega''_V} \left[ 2x_1(M'^2 + M_0'^2) - q^2 - P \cdot q \right. \\ & \left. \left. - 2(q^2 + P \cdot q) \frac{k'_\perp \cdot q_\perp}{q^2} - 2(m'_1 - m''_1)(m'_1 - m_2) \right] \right\}, \end{aligned} \quad (3.14)$$

$$\begin{aligned} a_+(q^2) = & \frac{N_c}{16\pi^3} \int dx_2 d^2 \vec{k}_\perp \frac{2h'_P h''_V}{x_2 \hat{N}'_1 \hat{N}''_1} \left\{ (x_1 - x_2)(x_2 m'_1 + x_1 m_2) - [2x_1 m_2 + m''_1 + (x_2 - x_1)m'_1] \frac{k'_\perp \cdot q_\perp}{q^2} \right. \\ & \left. - 2 \frac{x_2 q^2 + k'_\perp \cdot q_\perp}{x_2 q^2 \omega''_V} [k'_\perp \cdot k''_\perp + (x_1 m_2 + x_2 m'_1)(x_1 m_2 - x_2 m''_1)] \right\}, \end{aligned} \quad (3.15)$$

$$\begin{aligned} a_-(q^2) = & \frac{N_c}{16\pi^3} \int dx_2 d^2 \vec{k}_\perp \frac{h'_P h''_V}{x_2 \hat{N}'_1 \hat{N}''_1} \left\{ 2(2x_1 - 3)(x_2 m'_1 + x_1 m_2) - 8(m'_1 - m_2) \left[ \frac{k_\perp'^2}{q^2} + 2 \frac{(k'_\perp \cdot q_\perp)^2}{q^4} \right] \right. \\ & - [(14 - 12x_1)m'_1 - 2m''_1 - (8 - 12x_1)m_2] \frac{k'_\perp \cdot q_\perp}{q^2} + \frac{4}{\omega''_V} [(M'^2 + M''^2 - q^2 + 2(m'_1 - m_2)(m''_1 + m_2))] \\ & \times (A_3^2 + A_4^{(2)} - A_2^{(1)} + Z_2(3A_2^{(1)} - 2A_4^{(2)} - 1) + \frac{1}{2}P \cdot q(A_1^{(1)} + A_2^{(1)} - 1)[x_1(q^2 + P \cdot q) - 2M'^2 - 2k'_\perp \cdot q_\perp \\ & \left. - 2m'_1(m''_1 + m_2 - 2m_2(m'_1 - m_2))] \left[ \frac{k_\perp'^2}{q^2} + \frac{(k'_\perp \cdot q_\perp)^2}{q^4} \right] (4A_2^{(1)} - 3) \right\}, \end{aligned} \quad (3.16)$$

The form factors deduced by (axial-)vector currents defined in Eq. (3.2) can thus be evaluated by

$$\begin{aligned} V(q^2) &= -(M' + M'')g(q^2), \\ A_0(q^2) &= -\frac{1}{2M''}f(q^2) - \frac{M'^2 - M''^2}{2M''}a_+(q^2) - \frac{q^2}{2M''}a_-(q^2), \\ A_1(q^2) &= -f(q^2)/(M' + M''), \quad A_2(q^2) = (M' + M'')a_+(q^2). \end{aligned} \quad (3.17)$$

Analogously, we can obtain the concrete expressions of the (pseudo-)tensor form factors defined in Eq. (3.4) as [118]

$$\begin{aligned} T_1(q^2) = & \frac{N_c}{16\pi^3} \int dx_2 d^2 \vec{k}_\perp \frac{h'_P h''_V}{x_2 \hat{N}'_1 \hat{N}''_1} \left\{ 2A_1^{(1)}[M'^2 - M''^2 - 2m_1'^2 - 2\hat{N}'_1 + q^2 + 2(m'_1 m_2 + m''_1 m_2 - m'_1 m''_1)] \right. \\ & - 8A_1^{(2)} + (m'_1 + m''_1)^2 + \hat{N}'_1 + \hat{N}''_1 - q^2 + 4(M'^2 - M''^2)(A_2^{(2)} - A_3^{(2)}) + 4q^2(-A_1^{(1)} + A_2^{(1)} + A_3^{(2)} - A_4^{(2)}) \\ & \left. - \frac{4}{\omega''_V}(m'_1 + m''_1)A_1^{(2)} \right\}, \end{aligned} \quad (3.18)$$

$$\begin{aligned} T_2(q^2) = & T_1(q^2) + \frac{q^2}{M'^2 - M''^2} \frac{N_c}{16\pi^3} \int dx_2 d^2 \vec{k}_\perp \frac{h'_P h''_V}{x_2 \hat{N}'_1 \hat{N}''_1} \left\{ 2A_2^{(1)}[M'^2 - M''^2 - 2m_1'^2 - 2\hat{N}'_1 + q^2 \right. \\ & + 2(m'_1 m_2 + m''_1 m_2 - m'_1 m''_1)] - 8A_1^{(2)} - 2M'^2 + 2m_1'^2 + (m'_1 + m''_1)^2 + 2(m_2 - 2m'_1)m_2 + 3\hat{N}'_1 + \hat{N}''_1 \\ & - q^2 + 2Z_2 + 4(q^2 - 2M'^2 - 2M''^2)(A_2^{(2)} - A_3^{(2)}) - 4(M'^2 - M''^2)(-A_1^{(1)} + A_2^{(1)} + A_3^{(2)} - A_4^{(2)}) \\ & \left. - \frac{4}{\omega''_V}(m''_1 - m'_1 + 2m_2)A_1^{(2)} \right\}, \end{aligned} \quad (3.19)$$



$$\begin{aligned}
T_3(q^2) = & \frac{N_c}{16\pi^3} \int dx_2 d^2\vec{k}_\perp \frac{h'_P h''_V}{x_2 \hat{N}'_1 \hat{N}''_1} \left\{ -2A_2^{(1)} [M'^2 - M''^2 - 2m_1'^2 - 2\hat{N}'_1 + q^2 + 2(m'_1 m_2 + m'_1 m_2 - m'_1 m_1'')] \right. \\
& + 8A_1^{(2)} + 2M'^2 - 2m_1'^2 - (m'_1 + m_1'')^2 - 2(m_2 - 2m'_1)m_2 - 3\hat{N}'_1 - \hat{N}''_1 + q^2 - 2Z_2 - 4(q^2 - M'^2 - 3M''^2) \\
& \times (A_2^{(2)} - A_3^{(2)}) + \frac{4}{\omega_V''} ((m''_1 - m'_1 + 2m_2)[A_1^{(2)} + (M'^2 - M''^2)(A_2^{(2)} + A_3^{(2)} - A_1^{(1)})] \\
& \left. + (m'_1 + m_1'')(M'^2 - M''^2)(A_2^{(1)} - A_3^{(2)} - A_4^{(2)}) + m'_1(M'^2 - M''^2)(A_1^{(1)} + A_2^{(1)} - 1)) \right\}. \quad (3.20)
\end{aligned}$$

Following the treatment in Ref. [110], the  $h_M$  is taken as

$$\begin{aligned}
h'_P &= (M'^2 - M_0'^2) \sqrt{\frac{x_1 x_2}{N_c}} \frac{1}{\sqrt{2}\tilde{M}'_0} \phi_s(x_2, \vec{k}'_\perp), \\
h''_V &= (M''^2 - M_0''^2) \sqrt{\frac{x_1 x_2}{N_c}} \frac{1}{\sqrt{2}\tilde{M}''_0} \phi_s(x_2, \vec{k}''_\perp), \quad (3.21)
\end{aligned}$$

where  $\tilde{M}_0^{(\prime\prime)} = \sqrt{M_0^{(\prime\prime)2} - (m_1^{(\prime\prime)} - m_2)^2}$ , and  $\phi_s$  is the space wave function of the pseudoscalar or vector meson.

In the previous theoretical work [110, 140], the phenomenological Gaussian-type wave functions

$$\phi_s(x_2, \vec{k}_\perp^{(\prime\prime)}) = 4 \left( \frac{\pi}{\beta'^{(\prime\prime)2}} \right)^{3/4} \sqrt{\frac{e_1^{(\prime\prime)} e_2}{x_1 x_2 M_0'^{(\prime\prime)}}} \exp \left( -\frac{\vec{k}_\perp^{(\prime\prime)2} + k_z^{(\prime\prime)2}}{2\beta'^{(\prime\prime)2}} \right), \quad (3.22)$$

with

$$\begin{aligned}
k_z^{(\prime\prime)} &= \frac{x_2 M_0'^{(\prime\prime)}}{2} - \frac{m_2^2 + \vec{k}_\perp^{(\prime\prime)2}}{2x_2 M_0'^{(\prime\prime)}}, \\
e_1^{(\prime\prime)} &= \sqrt{m_1^{(\prime\prime)2} + \vec{k}_\perp^{(\prime\prime)2} + k_z^{(\prime\prime)2}}, \\
e_2 &= \sqrt{m_2^2 + \vec{k}_\perp^2 + k_z^2}, \quad (3.23)
\end{aligned}$$

are widely used. It inevitably introduces the dependence of the parameter  $\beta$ . The phenomenological parameter  $\beta$  can be fixed by the decay constant [109, 110, 118]. However, as we all know, the decay constant is only associated with the meson wave function at the endpoint  $q^2 = 0$ . This indicates that the simple wave function Eq. (3.22) deviating from the  $q^2 = 0$  region may be unreliable.

Taking advantage of the modified GI model [184], we can obtain the numerical spatial wave functions of the mesons concerned. By replacing the form in Eq. (3.22) with

$$\begin{aligned}
\phi_l(x_2, \vec{k}_\perp^{(\prime\prime)}) &= \sqrt{4\pi} \sum_{n=1}^{N_{\max}} c_n \sqrt{\frac{e_1^{(\prime\prime)} e_2}{x_1 x_2 M_0'^{(\prime\prime)}}} R_{nl} \left( \sqrt{\vec{k}_\perp^{(\prime\prime)2} + k_z^{(\prime\prime)2}} \right), \\
\phi_s(x_2, \vec{k}_\perp^{(\prime\prime)}) &\equiv \phi_{l=0}(x_2, \vec{k}_\perp^{(\prime\prime)}), \quad (3.24)
\end{aligned}$$

where  $c_n$  are the expansion coefficients of the corresponding eigenvectors and  $l$  is the orbital angular momentum of the meson, we can avoid the corresponding uncertainty. In Table III,

we collect the expansion coefficients  $c_n$  of the meson wave functions involved. In addition, the factor  $\sqrt{4\pi}$  is needed to satisfy the normalization:

$$\int \frac{dx_2 d^2\vec{k}_\perp}{2(2\pi)^3} \phi_l^*(x_2, \vec{k}_\perp) \phi_l(x_2, \vec{k}_\perp) = 1. \quad (3.25)$$

Besides, the  $R_{nl}$  is the SHO wave function as

$$R_{nl}(|p|) = \frac{(-1)^{n-1}}{\beta^{3/2}} \sqrt{\frac{2(n-1)!}{\Gamma(n+l+1/2)}} \left( \frac{p}{\beta} \right)^l \exp \left( -\frac{p^2}{2\beta^2} \right) L_{n-1}^l \left( \frac{p^2}{\beta^2} \right). \quad (3.26)$$

The parameter  $\beta = 0.5$  GeV in the above equation is consistent with Ref. [184].

## IV. NUMERICAL RESULTS AND DISCUSSIONS

### A. The form factors

With the input of the numerical wave functions, and the concrete expressions of the seven form factors in Eqs. (3.13)-(3.20), we present in this subsection the numerical results of  $B_c \rightarrow D_s^*$  form factors.

Following the approach described in Refs. [108, 110], we assume the condition  $q^+ = 0$ . This implies that our form factor calculations are performed in the spacelike region ( $q^2 < 0$ ), and therefore we need to extrapolate them to the timelike region ( $q^2 > 0$ ). To perform the analytical continuation, we utilize the  $z$ -series parametrization [127]

$$\begin{aligned}
\mathcal{F}(q^2) = & \frac{\mathcal{F}(0)}{1 - q^2/m_{\text{pole}}^2} \left\{ 1 + a_1 \left( z(q^2) - z(0) - \frac{1}{3} [z(q^2)^2 - z(0)^2] \right) \right. \\
& \left. + a_2 \left( z(q^2) - z(0) + \frac{2}{3} [z(q^2)^2 - z(0)^2] \right) \right\}, \quad (4.1)
\end{aligned}$$

where  $a_i$  ( $i=1,2$ ) are free parameters needed to fit in the  $q^2 < 0$  region, and the  $z(q^2)$  is taken as

$$z(q^2) = \frac{\sqrt{t_+ - q^2} - \sqrt{t_+ - t_0}}{\sqrt{t_+ - q^2} + \sqrt{t_+ - t_0}} \quad (4.2)$$

with  $t_\pm = (M' \pm M'')^2$  and  $t_0 = t_+ (1 - \sqrt{1 - t_-/t_+})$ .

TABLE III: The calculated masses and the expansion coefficients  $c_n$  of the wave function of the mesons involved [184]. The masses are given in the units of MeV.

States	Masses [184]	Experiments [172]	Eigenvector coefficients $c_n$ [184]
$B_c$	6271	$6274.47 \pm 0.32$	$\{0.7877, 0.4410, 0.2857, 0.1991, 0.1470, 0.1132, 0.0900, 0.0734, 0.0611, 0.0517, 0.0444, 0.0385, 0.0338, 0.0299, 0.0266, 0.0238, 0.0215, 0.0195, 0.0177, 0.0162, 0.0148, 0.0136, 0.0125, 0.0116, 0.0107, 0.0099, 0.0092, 0.0084, 0.0081, 0.0066, 0.0081\}$
$D_s^*$	2112	$2112.2 \pm 0.4$	$\{0.9708, 0.16203, 0.1515, 0.0605, 0.0518, 0.0286, 0.0240, 0.0156, 0.0130, 0.0093, 0.0078, 0.0059, 0.0050, 0.0039, 0.0033, 0.0027, 0.0023, 0.0019, 0.0016, 0.0013, 0.0012, 0.0010, 0.0008, 0.0007, 0.0006, 0.0005, 0.0005, 0.0004, 0.0003, 0.0003, 0.0003\}$

To determine the values of the free parameters  $a_i$ , as given in Eq. (4.1), we perform numerical calculations at 200 equally spaced points for each form factor, ranging from  $-20 \text{ GeV}^2$  to  $-0.1 \text{ GeV}^2$ , using Eqs. (3.13)-(3.20). The calculated points are then fitted using Eq. (4.1). The fitted values of the free parameters, as well as  $\mathcal{F}(0)$ ,  $\mathcal{F}(q_{\text{max}}^2)$ , and the pole masses, are listed in Table IV. Additionally, the  $q^2$  dependence of the transition form factors  $B_c \rightarrow D_s^*$  is shown in Fig. 3.

TABLE IV: Our results of the weak transition form factors of  $B_c \rightarrow D_s^*$  by using the covariant LFQM.

	$\mathcal{F}(0)$	$\mathcal{F}(q_{\text{max}}^2)$	$m_{\text{pole}} \text{ (GeV)}$	$a_1$	$a_2$
$V^{B_c \rightarrow B_s^*}$	0.434	1.652	5.415	-7.909	15.667
$A_0^{B_c \rightarrow B_s^*}$	0.387	1.436	5.367	-6.790	9.427
$A_1^{B_c \rightarrow B_s^*}$	0.274	0.588	5.829	-0.721	-4.299
$A_2^{B_c \rightarrow B_s^*}$	0.159	0.438	5.829	-4.942	5.168
$T_1^{B_c \rightarrow B_s^*}$	0.265	1.050	5.415	-8.821	19.272
$T_2^{B_c \rightarrow B_s^*}$	0.265	0.424	5.829	3.067	-9.950
$T_3^{B_c \rightarrow B_s^*}$	0.231	0.637	5.829	-4.985	4.566

In Table V, we compare our results for the  $B_c \rightarrow D_s^*$  weak transition form factors at the endpoint  $q^2 = 0$  with other approaches, in which the Refs. [102, 103] calculated the concerned form factors with the QCD sum rule, Refs. [100, 114, 140] used the covariant LFQM, and the Ref. [185] used the Bauer-Stech-Wirbel model and considered the effects of flavor dependence on the form factors caused by possible variation of the average transverse quark momentum ( $\omega$ ) inside the meson. In addition, Ref. [100] also used the CQM, and the Ref. [101] used the pQCD approach. Refs. [100, 101, 103] contain the results of (pseudo)-tensor form factors. Obviously, our results of the (pseudo)-tensor form factors, i.e.,  $T_{1,2,3}$ , at the endpoint  $q^2 = 0$  are consistent with the predictions of pQCD [101] and LFQM [100]. We expect further theoretical work, especially LQCD, which is useful to constrain the behavior of the form factors in low-recoiling region, to test our results.

## B. The angular distributions and physical observables

With the above preparations, in this subsection we present our numerical results of the branching fractions and some an-

gular observables, i.e., the  $CP$ -averaged normalized angular coefficients  $S_i$ , the lepton's forward-backward asymmetry parameter  $A_{FB}$ , the longitudinal (transverse) polarization fractions of the  $D_s^*$  meson  $F_{L(T)}$ . In addition, we also investigate the clean angular observables  $P_{1,2,3}$  and  $P'_{4,5,6,8}$ . The hadron and lepton masses are quoted from the PDG [172], as well as the lifetime  $\tau_{B_c} = 0.510\text{ps}$  and the branching fraction  $\mathcal{B}(D_s^* \rightarrow D_s \pi) = 5\%$ .

First, we focus on the angular coefficients  $S_i$  and  $A_i$  defined in Eq. (2.15). The  $q^2$  dependence of the normalized  $CP$ -averaged angular coefficients  $S_i$  are presented in Fig. 4, while the  $CP$  asymmetry angular coefficients  $A_i$  are shown in Fig. 5. The blue dashed lines and the magenta solid lines represent the muon and the tau channels, respectively. Since the electron channel shows similar behavior to the muon channel, we will only present our results for the muon and the tau channels here. In the energy regions of  $8.0 < q^2 < 11.0 \text{ GeV}^2$  and  $12.5 < q^2 < 15.0 \text{ GeV}^2$ , we use the gray areas to mark the charm loop contributions from the charmonium states  $J/\psi$  and  $\psi(2S)$ . In the experiment, these two regions are generally truncated. The  $CP$  asymmetry angular coefficients,  $A_i$ , are shown to be very small in the SM, due to the direct  $CP$  violation being proportional to the  $\text{Im}[V_{ub}V_{us}^*/V_{tb}V_{ts}^*]$ , which is around  $10^{-2}$ . This character is very clear in Fig. 5. Also, the  $S_{7,8,9}$  are also very small compared to the other angular coefficients  $S_i$ . These angular coefficients are important physical observables to reveal the underlying decay mechanism, and can be checked by future measurements at LHCb.

We further evaluate the  $CP$ -averaged differential branching fractions by using Eq. (2.16) and Eq. (2.17). The  $q^2$  dependence of the differential branching fractions are shown in Fig. 6, where the red, blue and magenta curves represent the  $e$ ,  $\mu$ , and  $\tau$  modes, respectively. The gray areas also denote the charm loop contributions from the charmonium states  $J/\psi$  and  $\psi(2S)$ . In Table VI, we present our result of the branching fractions and their ratios in different  $q^2$  bins. In the four  $q^2$  intervals, i.e.,  $[1.1, 6.0] \text{ GeV}^2$ ,  $[6.0, 8.0] \text{ GeV}^2$ ,  $[11.0, 12.5] \text{ GeV}^2$ , and  $[15.0, 17.0] \text{ GeV}^2$ , the branching fractions of the electron and muon modes can reach up to  $10^{-8}$ , and the ratio  $R^{e\mu} = 1$ , which is consistent with the SM prediction and reflects the LFU. In the high  $q^2$  region, that is  $[15.0, 17.0] \text{ GeV}^2$ , the branching fraction of the tau mode is on the order of magnitude of  $10^{-9}$ . We also obtain the ratio  $R^{\tau\mu} = 0.384$ . Combined with the branching fraction

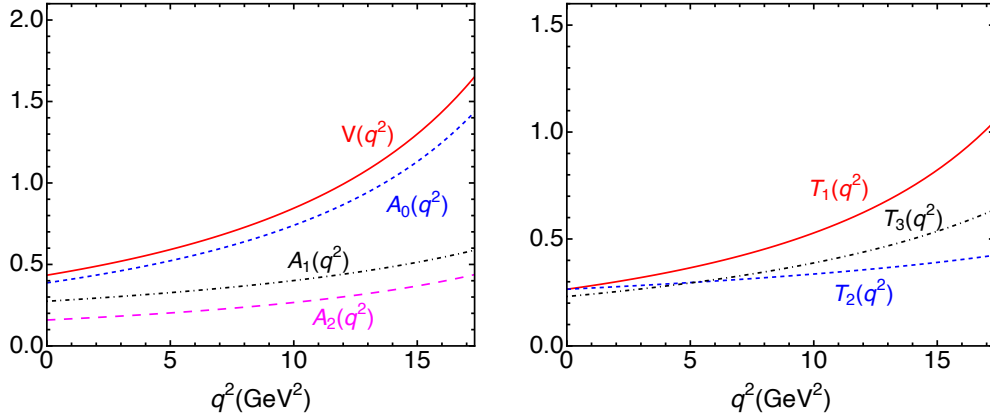


FIG. 3: The  $q^2$  dependence of the  $B_c \rightarrow D_s^*$  weak transition form factors. Here, the four dependent form factors deduced by (axial-)vector are presented in the left panel, while the three dependent ones deduced by (pseudo-)tensor are shown in the right panel.

TABLE V: Theoretical predictions of the  $B_c \rightarrow D_s^*$  transition form factors at the endpoint  $q^2 = 0$  using different approaches.

	$V^{B_c \rightarrow D_s^*}(0)$	$A_0^{B_c \rightarrow D_s^*}(0)$	$A_1^{B_c \rightarrow D_s^*}(0)$	$A_2^{B_c \rightarrow D_s^*}(0)$	$T_1^{B_c \rightarrow D_s^*}(0)$	$T_2^{B_c \rightarrow D_s^*}(0)$	$T_3^{B_c \rightarrow D_s^*}(0)$
This work	0.434	0.387	0.274	0.159	0.265	0.265	0.231
Ref. [102]	2.02	0.47	0.56	0.65	...	...	...
Ref. [185] <sup>[1]</sup>	0.032	0.016	0.015	0.013	...	...	...
Ref. [185] <sup>[2]</sup>	$0.29^{+0.02}_{-0.03}$	$0.16^{+0.01}_{-0.01}$	$0.18^{+0.01}_{-0.02}$	$0.20^{+0.02}_{-0.03}$	...	...	...
Ref. [114]	$0.23^{+0.04}_{-0.03}$	$0.17^{+0.01}_{-0.01}$	$0.14^{+0.02}_{-0.01}$	$0.12^{+0.02}_{-0.02}$	...	...	...
Ref. [140]	$0.25^{+0.00}_{-0.00}$	$0.18^{+0.02}_{-0.03}$	$0.16^{+0.01}_{-0.02}$	$0.15^{+0.01}_{-0.01}$	...	...	...
Ref. [100]	0.336	0.164	0.118	...	0.214	0.214	...
Ref. [100]	0.262	0.139	0.144	...	0.167	0.167	...
Ref. [103]	$0.54 \pm 0.018$	$0.30 \pm 0.017$	$0.36 \pm 0.013$	...	$0.31 \pm 0.017$	$0.33 \pm 0.016$	$0.29 \pm 0.034$
Ref. [101]	$0.33 \pm 0.06$	$0.21 \pm 0.04$	$0.23 \pm 0.04$	$0.25 \pm 0.05$	$0.28 \pm 0.06$	$0.28 \pm 0.06$	$0.27 \pm 0.06$

<sup>1</sup> These results, listed in the fourth row, are obtained by using the universe parameter  $\omega = 0.40$  GeV.

<sup>2</sup> These results, listed in the fifth row, are obtained by using different parameters, i.e.,  $\omega = 0.96^{+0.08}_{-0.07}$  GeV for the  $B_c$  meson and  $\omega = 0.51$  GeV for the  $D_s^*$  meson.

$\mathcal{B}(D_s^* \rightarrow D_s \pi) = 5\%$ , we have

$$\begin{aligned} \mathcal{B}(B_c \rightarrow D_s^* e^+ e^-)_{1.1 < q^2 < 6.0 \text{ GeV}^2} &= 1.25 \times 10^{-7}, \\ \mathcal{B}(B_c \rightarrow D_s^* \mu^+ \mu^-)_{1.1 < q^2 < 6.0 \text{ GeV}^2} &= 1.24 \times 10^{-7}, \end{aligned}$$

which may well be tested by the ongoing LHCb experiment.

TABLE VI: Our results of the branching fractions of  $B_c \rightarrow D_s^* (\rightarrow D_s \pi) \ell^+ \ell^-$  ( $\ell = e, \mu, \tau$ ) (in the units of  $10^{-8}$ ) in different  $q^2$  bins.

$q^2$ bins (GeV <sup>2</sup> )	$\mathcal{B}(\ell = e)$	$\mathcal{B}(\ell = \mu)$	$\mathcal{B}(\ell = \tau)$
[1.1, 6.0]	0.624	0.622	
		$R^{e\mu} = 1.00$	
[6.0, 8.0]	0.356	0.355	
		$R^{e\mu} = 1.00$	
[11.0, 12.5]	0.283	0.283	
		$R^{e\mu} = 1.00$	
[15.0, 17.0]	0.256	0.256	0.098
		$R^{e\mu} = 1.00, R^{\tau\mu} = 0.384$	

We also investigate the physical observables, i.e., the lepton forward-backward asymmetry parameter  $A_{FB}$  and the longitudinal (transverse) polarization fractions  $F_L(F_T)$ . The  $q^2$  dependence of these observables are presented in Fig. 7 and Fig. 8, respectively. Their averaged values in different  $q^2$  bins, defined by

$$\langle A \rangle \Big|_{q_{\min}^2}^{q_{\max}^2} = \frac{\int_{q_{\min}^2}^{q_{\max}^2} A[q^2] \left( \frac{d\Gamma}{dq^2} + \frac{d\bar{\Gamma}}{dq^2} \right) dq^2}{\int_{q_{\min}^2}^{q_{\max}^2} \left( \frac{d\Gamma}{dq^2} + \frac{d\bar{\Gamma}}{dq^2} \right) dq^2}, \quad (4.3)$$

where  $A = (A_{FB}, F_L, F_T)$ , are shown in Table VII.

In addition, we present our results for the  $q^2$  dependent clean angular observables  $P_{1,2,3}$  and  $P'_{4,5,6,8}$  in Fig. 9. In Ref. [22], the LHCb Collaboration reported the measurement of the form-factor-independent observables  $P'_{4,5,6,8}$  of the  $B^0 \rightarrow K^{*0} \mu^+ \mu^-$  decay. In particular, in the interval of  $4.30 < q^2 < 8.68$  GeV<sup>2</sup>, the observable  $P'_5$  shows  $3.7 \sigma$  discrepancy with the SM prediction [23]. After integration over the energy region  $1.0 < q^2 < 6.0$  GeV<sup>2</sup>, the discrepancy is determined to be  $2.5 \sigma$ . So we want to investigate these clean angular observables in the rare semileptonic decay of bottom-

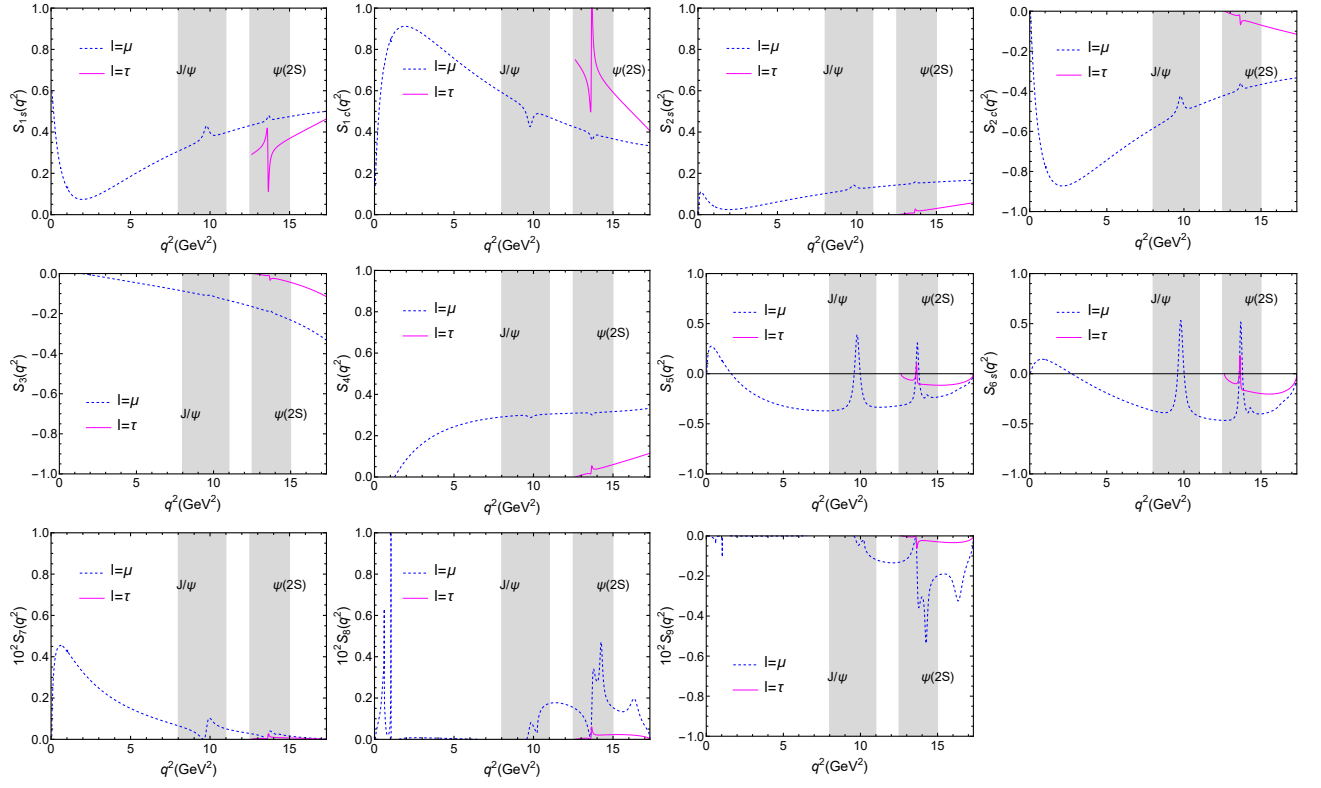


FIG. 4: The  $q^2$  dependence of normalized  $CP$ -averaged angular coefficients  $S_i$ , where the blue dashed and magenta solid curves are our results for the  $\mu$  and  $\tau$  modes, respectively.

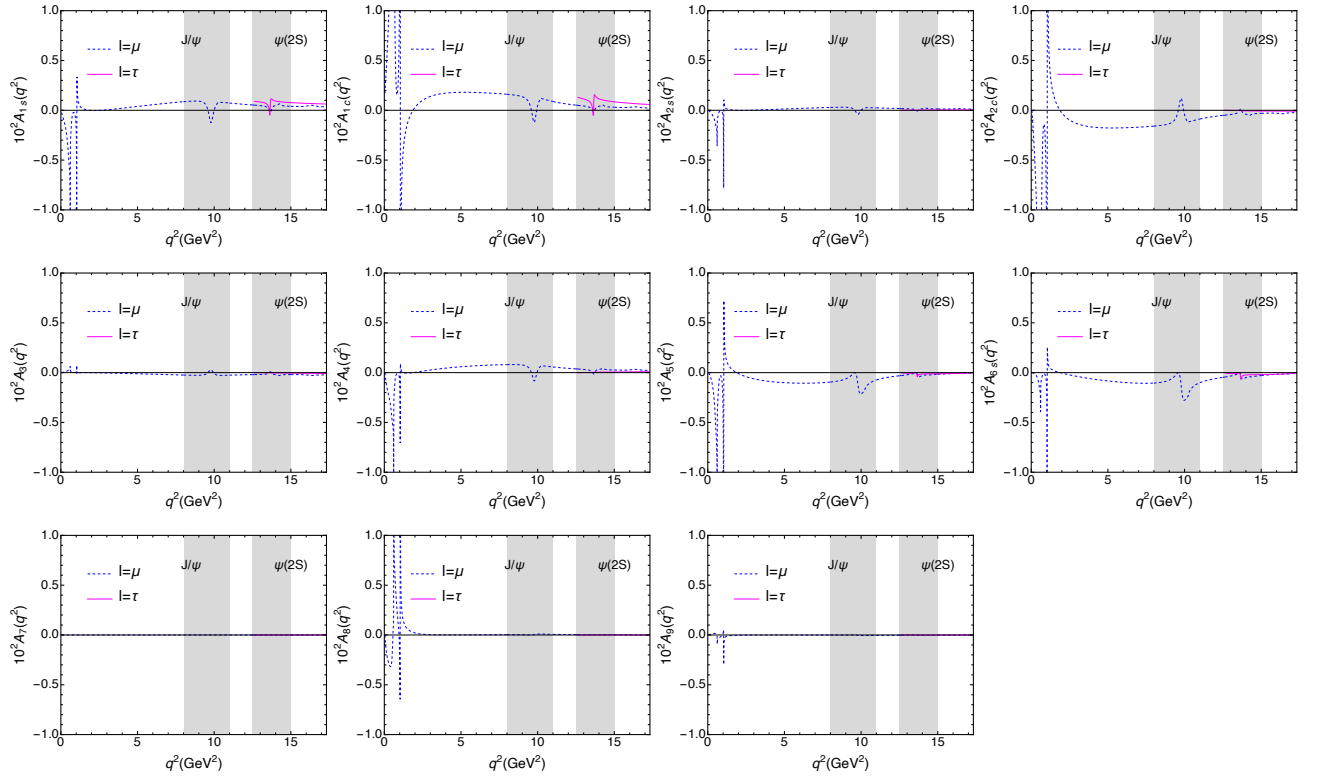


FIG. 5: The  $q^2$  dependence of normalized  $CP$  asymmetry angular coefficients  $A_i$ , where the blue dashed and magenta solid curves are our results for the  $\mu$  and  $\tau$  modes, respectively.

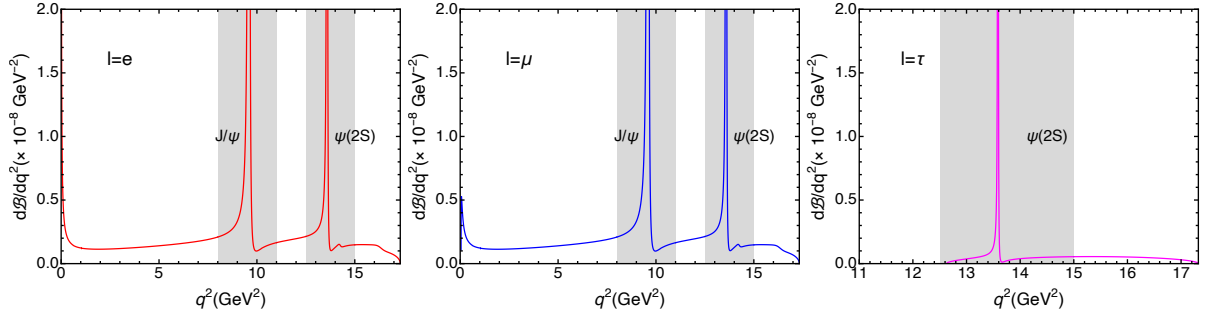


FIG. 6: The  $q^2$  dependence of differential branching fractions  $\mathcal{B}(B_c \rightarrow D_s^*(\rightarrow D_s \pi) \ell^+ \ell^-)$  [ $\ell=e$  (left panel),  $\mu$  (center panel), and  $\tau$  (right panel)], where the red, blue, and magenta curves are our results for the  $e$ ,  $\mu$ , and  $\tau$  modes, respectively.

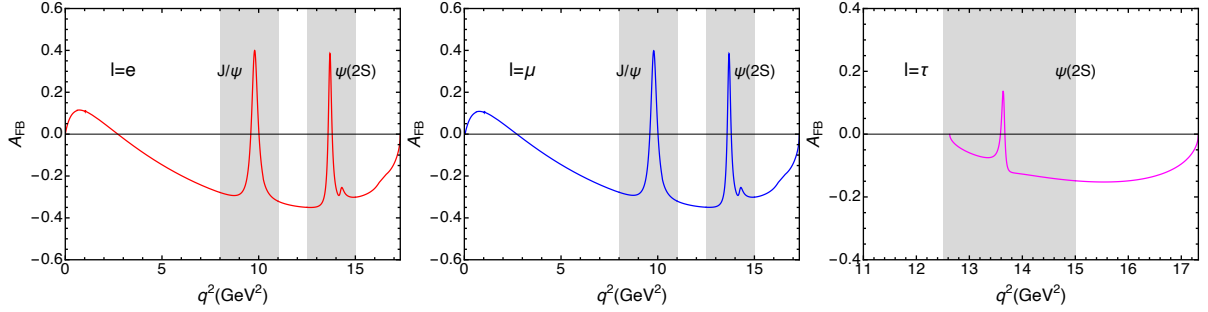


FIG. 7: The  $q^2$  dependence of lepton forward-backward asymmetry parameter  $A_{FB}$  in  $B_c \rightarrow D_s^*(\rightarrow D_s \pi) \ell^+ \ell^-$  [ $\ell=e$  (left panel),  $\mu$  (center panel), and  $\tau$  (right panel)] processes, where the red, the blue, and the magenta curves are our results from the  $e$ ,  $\mu$ , and  $\tau$  modes, respectively.

TABLE VII: The averaged forward-backward asymmetry  $\langle A_{FB} \rangle$  and the longitudinal (transverse) polarization fractions  $\langle F_L \rangle$  ( $\langle F_T \rangle$ ) in different  $q^2$  bins.

$q^2$ bins (GeV $^2$ )	$\langle A_{FB}(\ell=e) \rangle$	$\langle A_{FB}(\ell=\mu) \rangle$	$\langle A_{FB}(\ell=\tau) \rangle$
[1.1, 6.0]	-0.061	-0.061	
[6.0, 8.0]	-0.243	-0.242	
[11.0, 12.5]	-0.340	-0.339	
[15.0, 17.0]	-0.254	-0.254	-0.143
$q^2$ bins (GeV $^2$ )	$\langle F_L(\ell=e) \rangle$	$\langle F_L(\ell=\mu) \rangle$	$\langle F_L(\ell=\tau) \rangle$
[1.1, 6.0]	0.815	0.817	
[6.0, 8.0]	0.637	0.638	
[11.0, 12.5]	0.446	0.446	
[15.0, 17.0]	0.352	0.352	0.410
$q^2$ bins (GeV $^2$ )	$\langle F_T(\ell=e) \rangle$	$\langle F_T(\ell=\mu) \rangle$	$\langle F_T(\ell=\tau) \rangle$
[1.1, 6.0]	0.185	0.183	
[6.0, 8.0]	0.363	0.362	
[11.0, 12.5]	0.554	0.554	
[15.0, 17.0]	0.648	0.648	0.590

charmed meson. In order to exclude the charmonium contributions and make it easy to check experimentally, we also present the averaged values of these observables in different  $q^2$  intervals in Table VIII. The averaged value in a  $q^2$  bin is defined by Eq. (4.3).

In general, this quasi-four-body decay provides a set of

physical observables to study the corresponding weak interaction, and in particular the ratios of the branching fractions  $R^{e\mu}$  and  $R^{\tau\mu}$ , as well as the clean angular coefficients  $P_i$  and  $P'_i$ , can be helpful to search for the NP effects beyond the SM. We call for the ongoing LHCb experiment to search for this process and to measure the corresponding physical observables.

## V. SUMMARY

In this work, we have studied the  $B_c \rightarrow D_s^*$  transition form factors deduced by the (axial-)vector and (pseudo-)tensor currents, and, in the future, investigate the angular distributions of the quasi-four-body processes  $B_c \rightarrow D_s^*(\rightarrow D_s \pi) \ell^+ \ell^-$  ( $\ell=e, \mu, \tau$ ).

To describe the weak process, the relevant 7 independent form factors are calculated by utilizing the covariant LFQM approach. The concerned meson wave functions are adopted as the numerical wave functions, which are extracted from the solution of the modified GI model. This treatment avoids the  $\beta$  dependence and thus reduces the corresponding uncertainty. Our results of form factors are compared with other approaches. In particular, for the (pseudo-)tensor currents deduced form factors  $T_{1,2,3}(q^2=0)$ , our results agree with the pQCD prediction. More theoretical works, especially the LQCD and QCD sum rule (or light-cone sum rule) calculation, are highly appreciated to test our result and to refine the corresponding topic.

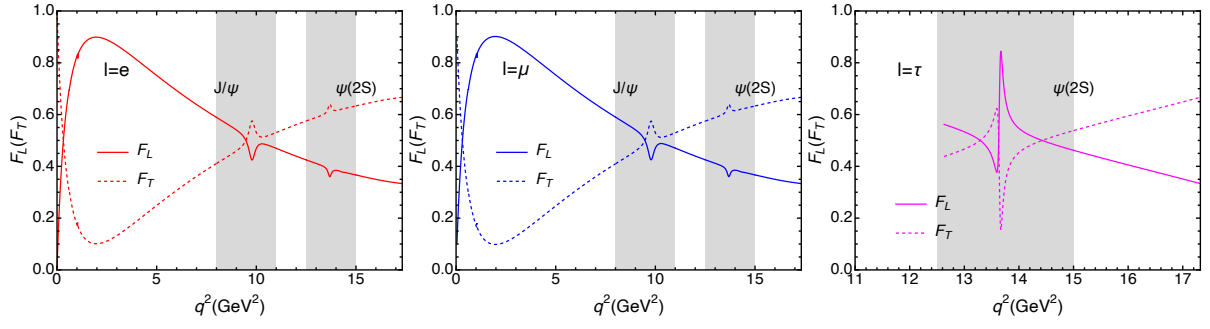


FIG. 8: The  $q^2$  dependence of  $D_s^*$  longitudinal (transverse) polarization fractions  $F_L(F_T)$  in  $B_c \rightarrow D_s^*(\rightarrow D_s\pi)\ell^+\ell^-$  [ $\ell=e$  (left panel),  $\mu$  (center panel), and  $\tau$  (right panel)] processes, where the red, the blue, and the magenta curves are our results from the  $e$ ,  $\mu$ , and  $\tau$  modes, respectively, and the solid and dashed curves represent the  $F_L$  and  $F_T$ , respectively.

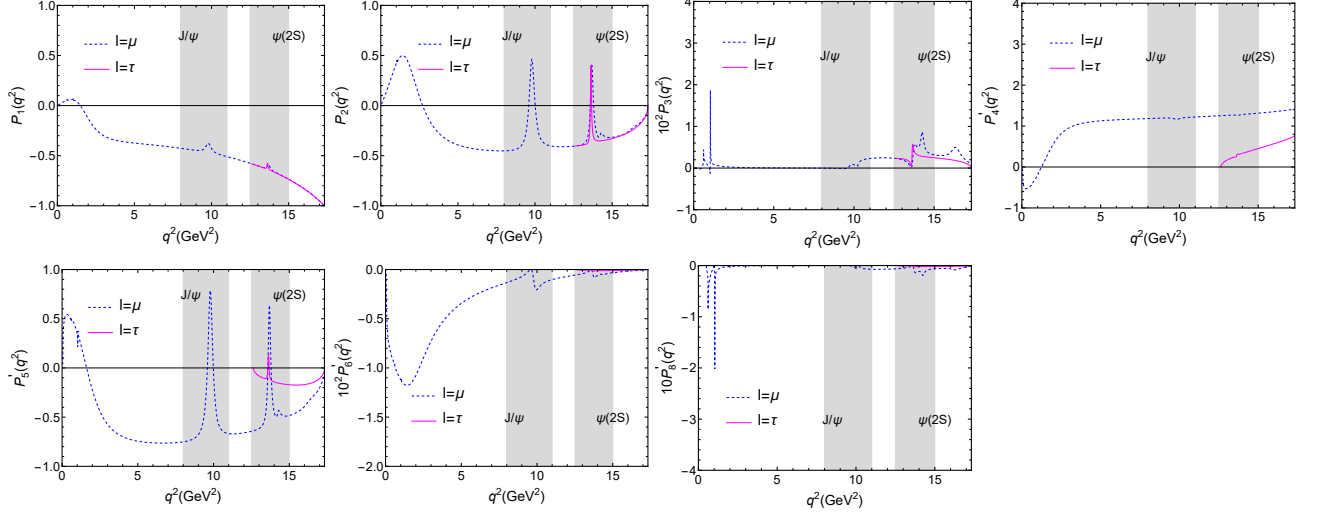


FIG. 9: The  $q^2$  dependence of the clean angular observables  $P_{1,2,3}$  and  $P'_{4,5,6,8}$ , where the blue dashed and magenta solid curves represent our results for the  $\mu$  and  $\tau$  modes, respectively.

With the obtained form factors, the rare semileptonic decays  $B_c \rightarrow D_s^*(\rightarrow D_s\pi)\ell^+\ell^-$  are studied. Not only the branching fractions, the lepton-side forward-backward asymmetry parameter  $A_{FB}$ , and the longitudinal and transverse polarization fractions  $F_L$  and  $F_T$ , but also the angular coefficients  $S_i$  and  $A_i$  are investigated. Numerically, the concerned cascade decays with  $e$  or  $\mu$  final states are around  $10^{-8}$ , which need to be tested by other approaches and ongoing experiments. In addition, the ratios of the branching fractions are also calculated to validate whether or not the LFU violated. Furthermore, the clean coefficient observables  $P_i$  and  $P'_j$  are presented, which reduce the uncertainty from the form factors and can be a possible signal to search for the NP effects.

Overall, in this work we have systematically studied the angular distribution of  $B_c \rightarrow D_s^*(\rightarrow D_s\pi)\ell^+\ell^-$  ( $\ell = e, \mu, \tau$ ) with

the form factors obtained by covariant LFQM. We live in the hope that with the completion of the LHCb experiment prepared for the Run 3 and Run 4 of the LHC and the improvement of the experimental capabilities, this rare semileptonic process can be discovered and we expect that the predicted physical observables can be tested.

#### Appendix A: The weak transition matrix elements deduced by axial-vector and (pseudo-)tensor currents

In this appendix, we present the concerned expressions of the weak transition matrix elements deduced by axial-vector current, and (pseudo-)tensor currents. The expression of axial-vector current matrix element is



TABLE VIII: The averaged values of the clean angular observables  $P_{1,2,3}$  and  $P'_{4,5,6,8}$  in different  $q^2$  bins.

$q^2$ bins (GeV <sup>2</sup> )	$\langle P_1(\ell = e) \rangle$	$\langle P_1(\ell = \mu) \rangle$	$\langle P_1(\ell = \tau) \rangle$	$q^2$ bins (GeV <sup>2</sup> )	$\langle P'_4(\ell = e) \rangle$	$\langle P'_4(\ell = \mu) \rangle$	$\langle P'_4(\ell = \tau) \rangle$
[1.1, 6.0]	-0.281	-0.281		[1.1, 6.0]	0.908	0.898	
[6.0, 8.0]	-0.408	-0.408		[6.0, 8.0]	1.177	1.169	
[11.0, 12.5]	-0.543	-0.543		[11.0, 12.5]	1.240	1.236	
[15.0, 17.0]	-0.822	-0.822	-0.826	[15.0, 17.0]	1.350	1.347	0.561
$q^2$ bins (GeV <sup>2</sup> )	$\langle P_2(\ell = e) \rangle$	$\langle P_2(\ell = \mu) \rangle$	$\langle P_2(\ell = \tau) \rangle$	$q^2$ bins (GeV <sup>2</sup> )	$\langle P'_5(\ell = e) \rangle$	$\langle P'_5(\ell = \mu) \rangle$	$\langle P'_5(\ell = \tau) \rangle$
[1.1, 6.0]	-0.125	-0.125		[1.1, 6.0]	-0.540	-0.534	
[6.0, 8.0]	-0.446	-0.446		[6.0, 8.0]	-0.766	-0.761	
[11.0, 12.5]	-0.409	-0.409		[11.0, 12.5]	-0.664	-0.662	
[15.0, 17.0]	-0.262	-0.262	-0.269	[15.0, 17.0]	-0.390	-0.390	-0.163
$q^2$ bins (GeV <sup>2</sup> )	$10^3 \langle P_3(\ell = e) \rangle$	$10^3 \langle P_3(\ell = \mu) \rangle$	$10^3 \langle P_3(\ell = \tau) \rangle$	$q^2$ bins (GeV <sup>2</sup> )	$10^3 \langle P'_6(\ell = e) \rangle$	$10^3 \langle P'_6(\ell = \mu) \rangle$	$10^3 \langle P'_6(\ell = \tau) \rangle$
[1.1, 6.0]	0.184	0.184		[1.1, 6.0]	-6.440	-6.320	
[6.0, 8.0]	0.007	0.007		[6.0, 8.0]	-1.868	-1.856	
[11.0, 12.5]	2.421	2.421		[11.0, 12.5]	-0.771	-0.769	
[15.0, 17.0]	3.442	3.442	2.008	[15.0, 17.0]	-0.188	-0.188	-0.070
$q^2$ bins (GeV <sup>2</sup> )	$10^3 \langle P'_8(\ell = e) \rangle$	$10^3 \langle P'_8(\ell = \mu) \rangle$	$10^3 \langle P'_8(\ell = \tau) \rangle$	$q^2$ bins (GeV <sup>2</sup> )	$10^3 \langle P'_8(\ell = e) \rangle$	$10^3 \langle P'_8(\ell = \mu) \rangle$	$10^3 \langle P'_8(\ell = \tau) \rangle$
				[1.1, 6.0]	-1.196	-1.164	
				[6.0, 8.0]	-0.029	-0.029	
				[11.0, 12.5]	-7.054	-7.030	
				[15.0, 17.0]	-6.147	-6.137	-1.467

$$\begin{aligned}
S_{\mu\nu}^A = & \text{Tr} \left[ \left( \gamma_\nu - \frac{(p_1'' - p_2)_\nu}{W_V''} \right) (\not{p}_1'' + m_1'') \gamma_\mu \gamma_5 (\not{p}_1' + m_1') \gamma_5 (-\not{p}_2 + m_2) \right] \\
= & -2g_{\mu\nu} \left[ m_2(q^2 - N_1' - N_1'' - m_1'^2 - m_1''^2) - m_1'(M''^2 - N_1'' - N_2 - m_1''^2 - m_2^2) \right. \\
& - m_1''(M'^2 - N_1' - N_2 - m_1'^2 - m_2^2) - 2m_1'm_1''m_2 \left. \right] - 8p_{1\mu}'p_{1\nu}'(m_2 - m_1') \\
& + 2m_1'(P_\mu q_\nu + P_\nu q_\mu + 2q_\mu q_\nu) - 2p_{1\mu}'P_\nu(m_1' - m_1'') - 2p_{1\nu}'P_\mu(m_1' + m_1'') \\
& - 2p_{1\mu}'q_\nu(3m_1' - m_1'' - 2m_2) - 2p_{1\nu}'q_\mu(3m_1' + m_1'' - 2m_2) \\
& - \frac{1}{2W_V''} \left[ 2p_{1\mu}'(M'^2 + M''^2 - q^2 - 2N_2 + 2(m_1' - m_2)(m_1'' + m_2)) \right. \\
& + q_\mu(q^2 - 2M'^2 + N_1' - N_1'' + 2N_2 - (m_1 + m_1'')^2 + 2(m_1' - m_2)^2) \\
& \left. + P_\mu(q^2 - N_1' - N_1'' - (m_1' + m_1'')^2) \right] (4p_{1\nu}' - 3q_\nu - P_\nu),
\end{aligned} \tag{A.1}$$

and the expression of (pseudo-)tensor current matrix element is

$$S_{\mu\nu}^{T+T5} = \text{Tr} \left[ \left( \gamma_\nu - \frac{(p_1'' - p_2)_\nu}{W_V''} \right) (\not{p}_1'' + m_1'') i\sigma_{\mu\delta} (1 + \gamma_5) q^\delta (\not{p}_1' + m_1') \gamma_5 (-\not{p}_2 + m_2) \right]. \tag{A.2}$$

By using the identity  $2\sigma_{\mu\delta}\gamma_5 = -i\epsilon_{\mu\delta\alpha\beta}\sigma^{\alpha\beta}$ , the matrix element  $S_{\mu\nu}^{T+T5}$  can be decomposed into

$$S_{\mu\nu}^{T+T5} = iq^\delta S_{\mu\nu\delta} + \frac{1}{2}\epsilon_{\mu\delta\alpha\beta}q^\delta S_{\nu}^{\alpha\beta}, \tag{A.3}$$

where  $iq^\delta S_{\mu\nu\delta}$  and  $\frac{1}{2}\epsilon_{\mu\delta\alpha\beta}q^\delta S_\nu^{\alpha\beta}$  are expressed as

$$\begin{aligned}
iq^\delta S_{\mu\nu\delta} &= \text{Tr}\left[\left(\gamma_\nu - \frac{(p_1'' - p_2)_\nu}{W_V''}\right)(\not{p}_1'' + m_1'')i\sigma_{\mu\delta}q^\delta(\not{p}_1' + m_1')\gamma_5(-\not{p}_2 + m_2)\right] \\
&= i\epsilon_{\mu\nu\alpha\beta}P^\alpha p_1^\beta(m_1'^2 - m_1''^2 + N_1' - N_1'') - \frac{i}{2}\epsilon_{\mu\nu\alpha\beta}P^\alpha q^\beta(m_1'^2 + 4m_1'm_1'' - m_1''^2 + N_1' - N_1'' + q^2) \\
&\quad - i\epsilon_{\mu\nu\alpha\beta}p_1^\alpha q^\beta(M'^2 - m_1'^2 + 4m_2(m_1' + m_1'') - 4m_1'm_1'' - m_1''^2 - 2m_2^2 + M''^2 - N_1' - N_1'' - 2N_2 - q^2) \\
&\quad + i\epsilon_{\mu\alpha\beta\gamma}P^\alpha p_1^\beta q^\gamma P_\nu\left(\frac{m_1' + m_1''}{W_V''}\right) + i\epsilon_{\mu\alpha\beta\gamma}P^\alpha p_1^\beta q^\gamma p_{1\nu}\left(2 - \frac{4(m_1' + m_1'')}{W_V''}\right) + i\epsilon_{\mu\alpha\beta\gamma}P^\alpha p_1^\beta q^\gamma q_\nu\left(\frac{3(m_1' + m_1'')}{W_V''} - 1\right) \\
&\quad - i\epsilon_{\nu\alpha\beta\gamma}P^\alpha p_1^\beta q^\gamma q_\mu + 2i\epsilon_{\nu\alpha\beta\gamma}P^\alpha p_1^\beta q^\gamma p_{1\mu},
\end{aligned} \tag{A.4}$$

$$\begin{aligned}
\frac{1}{2}\epsilon_{\mu\delta\alpha\beta}q^\delta S_\nu^{\alpha\beta} &= \text{Tr}\left[\left(\gamma_\nu - \frac{(p_1'' - p_2)_\nu}{W_V''}\right)(\not{p}_1'' + m_1'')\frac{1}{2}\sigma^{\alpha\beta}\epsilon_{\mu\delta\alpha\beta}q^\delta(\not{p}_1' + m_1')\gamma_5(-\not{p}_2 + m_2)\right] \\
&= -2ig_{\mu\nu}\{M'^2[m_1'(m_1' - m_1'') - N_1''] + m_1'^3(m_2 - m_1'') + m_1'^2(m_2(m_1'' - m_2) + M''^2 - N_2) \\
&\quad + m_1'(m_1'^3 - m_1''^2 m_2 - m_1''(M''^2 + N_1' - N_1'') + m_2(N_1' - N_1'' - q^2)) - m_1'^3 m_2 + m_1''^2 m_2^2 \\
&\quad + m_1'^2 N_2 + m_1' m_2 N_1' - m_1' m_2 N_1'' + m_1' m_2 q^2 - m_2^2 N_1' + m_2^2 N_1'' + M''^2 N_1' - N_1' N_2 + N_1'' N_2\} \\
&\quad + iP_\mu P_\nu \left\{ \frac{(m_1' + m_1'')(m_1'^2 - m_1''^2 + N_1' - N_1'') + q^2(m_1' - m_1'')}{2W_V''} \right\} \\
&\quad + iq_\mu q_\nu \{-2M'^2 - m_1'^2 + 2m_1'm_1'' - 4m_1'm_2 + m_1''^2 + 2m_2^2 - N_1' + N_1'' + 2N_2 - q^2 \\
&\quad + \frac{3}{2W_V''}[2M'^2 m_1' - m_1'^3 + m_1'^2(m_1'' + 2m_2) + m_1'(m_1''^2 - 2M''^2 - N_1' + N_1'' - q^2) \\
&\quad - (m_1'' + 2m_2)(m_1''^2 - N_1' + N_1'' - q^2)]\} \\
&\quad + ip_{1\mu}p_{1\nu}\{-4M'^2 + 4M''^2 - 4q^2 + \frac{4}{W_V''}[(M'^2 - M''^2)(m_1' + m_1'') + q^2(-m_1' + m_1'' + 2m_2)]\} \\
&\quad + iP_\mu p_{1\nu}\{2m_1'^2 - 2m_1''^2 + 2N_1' - 2N_1'' + \frac{2}{W_V''}[q^2(m_1' - m_1'') - (m_1' + m_1'')(m_1'^2 - m_1''^2 + N_1' - N_1'')]\} \\
&\quad + iP_\nu p_{1\mu}\{2q^2 + \frac{1}{W_V''}[q^2(m_1' - m_1'' - 2m_2) - (M'^2 - M''^2)(m_1' + m_1'')]\} \\
&\quad + iP_\mu q_\nu\{-2m_1'^2 + 2m_1'm_1'' - 2N_1' + \frac{3}{2W_V''}[(m_1' + m_1'')(m_1'^2 - m_1''^2 + N_1' - N_1'') + q^2(m_1'' - m_1')]\} \\
&\quad + iP_\nu q_\mu\{-m_1'^2 + m_1''^2 - N_1' + N_1'' - q^2 + \frac{1}{2W_V''}[2M'^2 m_1' - m_1'^3 + m_1'^2(m_1'' + 2m_2) \\
&\quad + m_1'(m_1''^2 - 2M''^2 - N_1' + N_1'' - q^2) - (m_1'' + 2m_2)(m_1''^2 - N_1' + N_1'' - q^2)]\} \\
&\quad + ip_{1\mu}q_\nu\{4M'^2 - 4m_1'm_1'' + 4m_1'm_2 + 4m_1''m_2 - 4m_2^2 - 4N_2 + 2q^2 \\
&\quad + \frac{3}{W_V''}[q^2(m_1' - m_1'' - 2m_2) - (M'^2 - M''^2)(m_1' + m_1'')]\} \\
&\quad + ip_{1\nu}q_\mu\{2M'^2 + 2m_1'^2 - 2m_1''^2 - 2M''^2 + 2N_1' - 2N_1'' + 2q^2 - \frac{2}{W_V''}[2M'^2 m_1' - m_1'^3 + m_1'^2(m_1'' + 2m_2) \\
&\quad + m_1'(m_1''^2 - 2M''^2 - N_1' + N_1'' - q^2) - (m_1'' + 2m_2)(m_1''^2 - N_1' + N_1'' - q^2)]\},
\end{aligned} \tag{A.5}$$

respectively.

#### ACKNOWLEDGMENTS

This work is supported by the China National Funds for Distinguished Young Scientists under Grant No. 11825503,

the National Key Research and Development Program of China under Contract No. 2020YFA0406400, the 111 Project under Grant No. B20063, the National Natural Science Foundation of China under Grant Nos. 12247101 and 12247155,

- 
- [1] W. Altmannshofer and D. M. Straub, New physics in  $b \rightarrow s$  transitions after LHC run 1, *Eur. Phys. J. C* **75** (2015) no.8, 382.
- [2] S. Descotes-Genon, L. Hofer, J. Matias and J. Virto, Global analysis of  $b \rightarrow s\ell\ell$  anomalies, *JHEP* **06** (2016), 092.
- [3] T. Skwarnicki [CLEO], Update on  $b \rightarrow sy$  and  $b \rightarrow s\ell^+\ell^-$  from CLEO,
- [4] T. Affolder *et al.* [CDF], Search for the flavor-changing neutral current decays  $B^+ \rightarrow \mu^+\mu^-K^+$  and  $B^0 \rightarrow \mu^+\mu^-K^{*0}$ , *Phys. Rev. Lett.* **83** (1999), 3378-3383.
- [5] B. Aubert *et al.* [BaBar], Search for  $B^+ \rightarrow K^+\ell^+\ell^-$  and  $B^0 \rightarrow K^{*0}\ell^+\ell^-$ , [arXiv:hep-ex/0008059 [hep-ex]].
- [6] K. Abe *et al.* [Belle], Observation of the decay  $B \rightarrow K\ell^+\ell^-$ , *Phys. Rev. Lett.* **88** (2002), 021801.
- [7] A. Ishikawa *et al.* [Belle], Observation of  $B \rightarrow K^*\ell^+\ell^-$ , *Phys. Rev. Lett.* **91** (2003), 261601.
- [8] J. T. Wei *et al.* [Belle], Measurement of the Differential Branching Fraction and Forward-Backward Asymmetry for  $B \rightarrow K^{(*)}\ell^+\ell^-$ , *Phys. Rev. Lett.* **103** (2009), 171801.
- [9] S. Wehle *et al.* [Belle], Lepton-Flavor-Dependent Angular Analysis of  $B \rightarrow K^*\ell^+\ell^-$ , *Phys. Rev. Lett.* **118** (2017) no.11, 111801.
- [10] S. Choudhury *et al.* [BELLE], Test of lepton flavor universality and search for lepton flavor violation in  $B \rightarrow K\ell\ell$  decays, *JHEP* **03** (2021), 105.
- [11] A. Abdesselam *et al.* [Belle], Test of Lepton-Flavor Universality in  $B \rightarrow K^*\ell^+\ell^-$  Decays at Belle, *Phys. Rev. Lett.* **126** (2021) no.16, 161801.
- [12] B. Aubert *et al.* [BaBar], Evidence for the rare decay  $B \rightarrow K^*\ell^+\ell^-$  and measurement of the  $B \rightarrow K\ell^+\ell^-$  branching fraction, *Phys. Rev. Lett.* **91** (2003), 221802.
- [13] B. Aubert *et al.* [BaBar], Direct CP, Lepton Flavor and Isospin Asymmetries in the Decays  $B \rightarrow K^{(*)}\ell^+\ell^-$ , *Phys. Rev. Lett.* **102** (2009), 091803.
- [14] J. P. Lees *et al.* [BaBar], Measurement of Branching Fractions and Rate Asymmetries in the Rare Decays  $B \rightarrow K^{(*)}\ell^+\ell^-$ , *Phys. Rev. D* **86** (2012), 032012.
- [15] T. Aaltonen *et al.* [CDF], Observation of the Baryonic Flavor-Changing Neutral Current Decay  $\Lambda_b \rightarrow \Lambda\mu^+\mu^-$ , *Phys. Rev. Lett.* **107** (2011), 201802.
- [16] V. Khachatryan *et al.* [CMS], Angular analysis of the decay  $B^0 \rightarrow K^{*0}\mu^+\mu^-$  from pp collisions at  $\sqrt{s} = 8$  TeV, *Phys. Lett. B* **753** (2016), 424-448.
- [17] R. Aaij *et al.* [LHCb], Differential branching fraction and angular analysis of the  $B^+ \rightarrow K^+\mu^+\mu^-$  decay, *JHEP* **02** (2013), 105.
- [18] R. Aaij *et al.* [LHCb], Test of lepton universality using  $B^+ \rightarrow K^+\ell^+\ell^-$  decays, *Phys. Rev. Lett.* **113** (2014), 151601.
- [19] R. Aaij *et al.* [LHCb], Measurements of the S-wave fraction in  $B^0 \rightarrow K^+\pi^-\mu^+\mu^-$  decays and the  $B^0 \rightarrow K^{*0}(892)\mu^+\mu^-$  differential branching fraction, *JHEP* **11** (2016), 047 [erratum: *JHEP* **04** (2017), 142].
- [20] R. Aaij *et al.* [LHCb], Test of lepton universality with  $B^0 \rightarrow K^{*0}\ell^+\ell^-$  decays, *JHEP* **08** (2017), 055.
- [21] R. Aaij *et al.* [LHCb], Test of lepton universality in beauty-quark decays, *Nature Phys.* **18** (2022) no.3, 277-282.
- [22] R. Aaij *et al.* [LHCb], Measurement of Form-Factor-Independent Observables in the Decay  $B^0 \rightarrow K^{*0}\mu^+\mu^-$ , *Phys. Rev. Lett.* **111** (2013), 191801.
- [23] U. Egede, T. Hurth, J. Matias, M. Ramon and W. Reece, New observables in the decay mode  $\bar{B}_d \rightarrow \bar{K}^{*0}\ell^+\ell^-$ , *JHEP* **11** (2008), 032.
- [24] M. Bordone, G. Isidori and A. Pattori, On the Standard Model predictions for  $R_K$  and  $R_{K^*}$ , *Eur. Phys. J. C* **76** (2016) no.8, 440.
- [25] D. Acosta *et al.* [CDF], Search for the Decay  $B_s \rightarrow \mu^+\mu^-\phi$  in  $p\bar{p}$  Collisions at  $\sqrt{s} = 1.8$ -TeV, *Phys. Rev. D* **65** (2002), 111101.
- [26] T. Aaltonen *et al.* [CDF], Search for the Rare Decays  $B^+ \rightarrow \mu^+\mu^-K^+$ ,  $B^0 \rightarrow \mu^+\mu^-K^{*0}(892)$ , and  $B_s^0 \rightarrow \mu^+\mu^-\phi$  at CDF, *Phys. Rev. D* **79** (2009), 011104.
- [27] V. M. Abazov *et al.* [D0], Search for the rare decay  $B_s^0 \rightarrow \phi\mu^+\mu^-$  with the D0 detector, *Phys. Rev. D* **74** (2006), 031107.
- [28] T. Aaltonen *et al.* [CDF], Measurement of the Forward-Backward Asymmetry in the  $B \rightarrow K^{(*)}\mu^+\mu^-$  Decay and First Observation of the  $B_s^0 \rightarrow \phi\mu^+\mu^-$  Decay, *Phys. Rev. Lett.* **106** (2011), 161801.
- [29] R. Aaij *et al.* [LHCb], Differential branching fraction and angular analysis of the decay  $B_s^0 \rightarrow \phi\mu^+\mu^-$ , *JHEP* **07** (2013), 084.
- [30] R. Aaij *et al.* [LHCb], Angular analysis and differential branching fraction of the decay  $B_s^0 \rightarrow \phi\mu^+\mu^-$ , *JHEP* **09** (2015), 179.
- [31] R. Aaij *et al.* [LHCb], Branching Fraction Measurements of the Rare  $B_s^0 \rightarrow \phi\mu^+\mu^-$  and  $B_s^0 \rightarrow f_2'(1525)\mu^+\mu^-$  Decays, *Phys. Rev. Lett.* **127** (2021) no.15, 151801.
- [32] T. V. Dong *et al.* [Belle], Search for the decay  $B_0 \rightarrow K^{*0}\tau^+\tau^-$  at the Belle experiment, *Phys. Rev. D* **108** (2023) no.1, L011102.
- [33] C. Bouchard *et al.* [HPQCD], Rare decay  $B \rightarrow K\ell^+\ell^-$  form factors from lattice QCD, *Phys. Rev. D* **88** (2013) no.5, 054509 [erratum: *Phys. Rev. D* **88** (2013) no.7, 079901].
- [34] R. R. Horgan, Z. Liu, S. Meinel and M. Wingate, Lattice QCD calculation of form factors describing the rare decays  $B \rightarrow K^*\ell^+\ell^-$  and  $B_s \rightarrow \phi\ell^+\ell^-$ , *Phys. Rev. D* **89** (2014) no.9, 094501.
- [35] J. A. Bailey, A. Bazavov, C. Bernard, C. M. Bouchard, C. DeTar, D. Du, A. X. El-Khadra, J. Foley, E. D. Freeland and E. Gámiz, *et al.*  $B \rightarrow K\ell^+\ell^-$  Decay Form Factors from Three-Flavor Lattice QCD, *Phys. Rev. D* **93** (2016) no.2, 025026.
- [36] P. Ball and R. Zwicky,  $B_{d,s} \rightarrow \rho, \omega, K^*, \phi$  decay form-factors from light-cone sum rules revisited, *Phys. Rev. D* **71** (2005), 014029.
- [37] P. Ball and R. Zwicky, New results on  $B \rightarrow \pi, K, \eta$  decay form-factors from light-cone sum rules, *Phys. Rev. D* **71** (2005), 014015.
- [38] Y. L. Wu, M. Zhong and Y. B. Zuo,  $B_s, D_s \rightarrow \pi, K, \eta, \rho, K^*, \omega, \phi$  Transition Form Factors and Decay Rates with Extraction of the CKM parameters  $|V_{ub}|$ ,  $|V_{cs}|$ ,  $|V_{cd}|$ , *Int. J. Mod. Phys. A* **21** (2006), 6125-6172.
- [39] M. Bartsch, M. Beylich, G. Buchalla and D. N. Gao, Precision Flavour Physics with  $B \rightarrow K\nu\bar{\nu}$  and  $B \rightarrow K\ell^+\ell^-$ , *JHEP* **11** (2009), 011.
- [40] A. Bharucha, D. M. Straub and R. Zwicky,  $B \rightarrow V\ell^+\ell^-$  in the Standard Model from light-cone sum rules, *JHEP* **08** (2016), 098.

- [41] W. Cheng, X. G. Wu and H. B. Fu, Reconsideration of the  $B \rightarrow K^*$  transition form factors within the QCD light-cone sum rules, *Phys. Rev. D* **95** (2017) no.9, 094023.
- [42] J. Gao, C. D. Lü, Y. L. Shen, Y. M. Wang and Y. B. Wei, Precision calculations of  $B \rightarrow V$  form factors from soft-collinear effective theory sum rules on the light-cone, *Phys. Rev. D* **101** (2020) no.7, 074035.
- [43] C. Bobeth, G. Hiller and G. Piranishvili, CP Asymmetries in bar  $B \rightarrow \bar{K}^*(\rightarrow \bar{K}\pi)\ell\ell$  and Untagged  $\bar{B}_s, B_s \rightarrow \phi(\rightarrow K^+K^-)\ell\ell$  Decays at NLO, *JHEP* **07** (2008), 106.
- [44] R. H. Li, C. D. Lü and W. Wang, Transition form factors of  $B$  decays into  $p$ -wave axial-vector mesons in the perturbative QCD approach, *Phys. Rev. D* **79** (2009), 034014.
- [45] W. Wang, R. H. Li and C. D. Lü, Radiative charmless  $B_s \rightarrow V\gamma$  and  $B_s \rightarrow A\gamma$  decays in pQCD approach, [[arXiv:0711.0432](#)] [hep-ph].
- [46] R. H. Li, C. D. Lü and W. Wang, Branching Ratios, Forward-backward Asymmetry and Angular Distributions of  $B \rightarrow K_1\ell^+\ell^-$  Decays, *Phys. Rev. D* **79** (2009), 094024.
- [47] W. F. Wang and Z. J. Xiao, The semileptonic decays  $B/B_s \rightarrow (\pi, K)(\ell^+\ell^-, \ell\nu, \nu\bar{\nu})$  in the perturbative QCD approach beyond the leading-order, *Phys. Rev. D* **86** (2012), 114025.
- [48] W. F. Wang, Y. Y. Fan, M. Liu and Z. J. Xiao, Semileptonic decays  $B/B_s \rightarrow (\eta, \eta', G)(\ell^+\ell^-, \ell\bar{\nu}, \nu\bar{\nu})$  in the perturbative QCD approach beyond the leading order, *Phys. Rev. D* **87** (2013) no.9, 097501.
- [49] Z. J. Xiao and X. Liu, The two-body hadronic decays of  $B_c$  meson in the perturbative QCD approach: A short review, *Chin. Sci. Bull.* **59** (2014), 3748-3759.
- [50] S. P. Jin, X. Q. Hu and Z. J. Xiao, Study of  $B_s \rightarrow K^{(*)}\ell^+\ell^-$  decays in the PQCD factorization approach with lattice QCD input, *Phys. Rev. D* **102** (2020) no.1, 013001.
- [51] S. P. Jin and Z. J. Xiao, Study of  $B_s \rightarrow \phi\ell^+\ell^-$  Decays in the PQCD Factorization Approach with Lattice QCD Input, *Adv. High Energy Phys.* **2021** (2021), 3840623.
- [52] A. Deandrea and A. D. Polosa, The Exclusive  $B_s \rightarrow \phi\mu^+\mu^-$  process in a constituent quark model, *Phys. Rev. D* **64** (2001), 074012.
- [53] C. Q. Geng and C. C. Liu, Study of  $B_s \rightarrow (\eta, \eta', \phi)\ell\bar{\ell}$  decays, *J. Phys. G* **29** (2003), 1103-1118.
- [54] C. H. Chen, C. Q. Geng and W. Wang, Z-mediated charge and CP asymmetries and FCNCs in  $B_{d,s}$  processes, *JHEP* **11** (2010), 089.
- [55] R. H. Li, C. D. Lü and W. Wang, Branching ratios, forward-backward asymmetries and angular distributions of  $B \rightarrow K_s^*\ell^+\ell^-$  in the standard model and new physics scenarios, *Phys. Rev. D* **83** (2011), 034034.
- [56] S. Dubnička, A. Z. Dubničková, A. Issadykov, M. A. Ivanov, A. Liptaj and S. K. Sakhiyev, Decay  $B_s \rightarrow \phi\ell^+\ell^-$  in covariant quark model, *Phys. Rev. D* **93** (2016) no.9, 094022.
- [57] N. R. Soni, A. Issadykov, A. N. Gadaria, J. J. Patel and J. N. Pandya, Rare  $b \rightarrow d$  decays in covariant confined quark model, *Eur. Phys. J. A* **58** (2022) no.3, 39.
- [58] A. Issadykov,  $B_s^0 \rightarrow \bar{K}^*(892)^0\ell^+\ell^-$  Decay in Covariant Confined Quark Model, *Phys. Part. Nucl. Lett.* **19** (2022) no.5, 460-462.
- [59] C. D. Lü and W. Wang, Analysis of  $B \rightarrow K_s^*(\rightarrow K\pi)\mu^+\mu^-$  in the higher kaon resonance region, *Phys. Rev. D* **85** (2012), 034014.
- [60] M. Ahmady, S. Keller, M. Thibodeau and R. Sandapen, Re-examination of the rare decay  $B_s \rightarrow \phi\mu^+\mu^-$  using holographic light-front QCD, *Phys. Rev. D* **100** (2019) no.11, 113005.
- [61] S. P. Li, X. Q. Li, Y. D. Yang and X. Zhang,  $R_{D^{(*)}}, R_{K^{(*)}}$  and neutrino mass in the 2HDM-III with right-handed neutrinos, *JHEP* **09** (2018), 149.
- [62] B. Barman, D. Borah, L. Mukherjee and S. Nandi, Correlating the anomalous results in  $b \rightarrow s$  decays with inert Higgs doublet dark matter and muon ( $g-2$ ), *Phys. Rev. D* **100** (2019) no.11, 115010.
- [63] L. Delle Rose, S. Khalil, S. J. D. King and S. Moretti,  $R_K$  and  $R_{K^*}$  in an Aligned 2HDM with Right-Handed Neutrinos, *Phys. Rev. D* **101** (2020) no.11, 115009.
- [64] A. Ordell, R. Pasechnik, H. Serôdio and F. Nottensteiner, Classification of anomaly-free 2HDMs with a gauged  $U(1)'$  symmetry, *Phys. Rev. D* **100** (2019) no.11, 115038.
- [65] C. Marzo, L. Marzola and M. Raidal, Common explanation to the  $R_{K^{(*)}}, R_{D^{(*)}}$  and  $\epsilon'/\epsilon$  anomalies in a 3HDM+ $\nu_R$  and connections to neutrino physics, *Phys. Rev. D* **100** (2019) no.5, 055031.
- [66] M. J. Aslam, C. D. Lü and Y. M. Wang,  $B \rightarrow K_0^*(1430)\ell^+\ell^-$  decays in supersymmetric theories, *Phys. Rev. D* **79** (2009), 074007.
- [67] S. Trifinopoulos,  $B$ -physics anomalies: The bridge between R-parity violating supersymmetry and flavored dark matter, *Phys. Rev. D* **100** (2019) no.11, 115022.
- [68] A. Shaw, Looking for  $B \rightarrow X_s\ell^+\ell^-$  in a nonminimal universal extra dimensional model, *Phys. Rev. D* **99** (2019) no.11, 115030.
- [69] W. Altmannshofer, S. Gori, M. Pospelov and I. Yavin, Quark flavor transitions in  $L_\mu - L_\tau$  models, *Phys. Rev. D* **89** (2014), 095033.
- [70] B. Bhattacharya, A. Datta, D. London and S. Shivashankara, Simultaneous Explanation of the  $R_K$  and  $R(D^{(*)})$  Puzzles, *Phys. Lett. B* **742** (2015), 370-374.
- [71] A. Crivellin, G. D'Ambrosio and J. Heeck, Addressing the LHC flavor anomalies with horizontal gauge symmetries, *Phys. Rev. D* **91** (2015) no.7, 075006.
- [72] A. Celis, J. Fuentes-Martin, M. Jung and H. Serodio, Family nonuniversal  $Z'$  models with protected flavor-changing interactions, *Phys. Rev. D* **92** (2015) no.1, 015007.
- [73] A. Falkowski, M. Nardecchia and R. Ziegler, Lepton Flavor Non-Universality in  $B$ -meson Decays from a  $U(2)$  Flavor Model, *JHEP* **11** (2015), 173.
- [74] B. Bhattacharya, A. Datta, J. P. Guévin, D. London and R. Watanabe, Simultaneous Explanation of the  $R_K$  and  $R_{D^{(*)}}$  Puzzles: a Model Analysis, *JHEP* **01** (2017), 015.
- [75] C. W. Chiang, X. G. He, J. Tandean and X. B. Yuan,  $R_{K^{(*)}}$  and related  $b \rightarrow s\ell\bar{\ell}$  anomalies in minimal flavor violation framework with  $Z'$  boson, *Phys. Rev. D* **96** (2017) no.11, 115022.
- [76] S. F. King, Flavourful  $Z'$  models for  $R_{K^{(*)}}$ , *JHEP* **08** (2017), 019.
- [77] A. Falkowski, S. F. King, E. Perdomo and M. Pierre, Flavourful  $Z'$  portal for vector-like neutrino Dark Matter and  $R_{K^{(*)}}$ , *JHEP* **08** (2018), 061.
- [78] B. C. Allanach, J. M. Butterworth and T. Corbett, Collider constraints on  $Z'$  models for neutral current B-anomalies, *JHEP* **08** (2019), 106.
- [79] S. Dwivedi, D. Kumar Ghosh, A. Falkowski and N. Ghosh, Associated  $Z'$  production in the flavorful  $U(1)$  scenario for  $R_{K^{(*)}}$ , *Eur. Phys. J. C* **80** (2020) no.3, 263.
- [80] B. Capdevila, A. Crivellin, C. A. Manzari and M. Montull, Explaining  $b \rightarrow s\ell^+\ell^-$  and the Cabibbo angle anomaly with a vector triplet, *Phys. Rev. D* **103** (2021) no.1, 015032.
- [81] J. H. Sheng, The Analysis of  $b \rightarrow s\ell^+\ell^-$  in the Family Non-Universal  $Z'$  Model, *Int. J. Theor. Phys.* **60** (2021) no.1, 26-46.
- [82] G. Hiller and M. Schmaltz,  $R_K$  and future  $b \rightarrow s\ell\ell$  physics beyond the standard model opportunities, *Phys. Rev. D* **90** (2014), 054014.

- [83] B. Gripaios, M. Nardecchia and S. A. Renner, Composite leptoquarks and anomalies in  $B$ -meson decays, JHEP **05** (2015), 006.
- [84] I. de Medeiros Varzielas and G. Hiller, Clues for flavor from rare lepton and quark decays, JHEP **06** (2015), 072.
- [85] D. Bečirević and O. Sumensari, A leptoquark model to accommodate  $R_K^{\text{exp}} < R_K^{\text{SM}}$  and  $R_{K^*}^{\text{exp}} < R_{K^*}^{\text{SM}}$ , JHEP **08** (2017), 104.
- [86] L. Di Luzio, A. Greljo and M. Nardecchia, Gauge leptoquark as the origin of  $B$ -physics anomalies, Phys. Rev. D **96** (2017) no.11, 115011.
- [87] D. Bečirević, I. Doršner, S. Fajfer, N. Košnik, D. A. Faroughy and O. Sumensari, Scalar leptoquarks from grand unified theories to accommodate the  $B$ -physics anomalies, Phys. Rev. D **98** (2018) no.5, 055003.
- [88] A. Angelescu, D. Bečirević, D. A. Faroughy and O. Sumensari, Closing the window on single leptoquark solutions to the  $B$ -physics anomalies, JHEP **10** (2018), 183.
- [89] C. Cornella, J. Fuentes-Martin and G. Isidori, Revisiting the vector leptoquark explanation of the  $B$ -physics anomalies, JHEP **07** (2019), 168.
- [90] O. Popov, M. A. Schmidt and G. White,  $R_2$  as a single leptoquark solution to  $R_{D^{(*)}}$  and  $R_{K^{(*)}}$ , Phys. Rev. D **100** (2019) no.3, 035028.
- [91] L. Da Rold and F. Lamagna, A vector leptoquark for the  $B$ -physics anomalies from a composite GUT, JHEP **12** (2019), 112.
- [92] C. Hati, J. Kriewald, J. Orloff and A. M. Teixeira, A nonunitary interpretation for a single vector leptoquark combined explanation to the  $B$ -decay anomalies, JHEP **12** (2019), 006.
- [93] A. Datta, J. L. Feng, S. Kamali and J. Kumar, Resolving the  $(g-2)_\mu$  and  $B$  Anomalies with Leptoquarks and a Dark Higgs Boson, Phys. Rev. D **101** (2020) no.3, 035010.
- [94] S. Balaji and M. A. Schmidt, Unified SU(4) theory for the  $R_{D^{(*)}}$  and  $R_{K^{(*)}}$  anomalies, Phys. Rev. D **101** (2020) no.1, 015026.
- [95] A. Crivellin, D. Müller and F. Saturnino, Flavor Phenomenology of the Leptoquark Singlet-Triplet Model, JHEP **06** (2020), 020.
- [96] S. Saad, Combined explanations of  $(g-2)_\mu$ ,  $R_{D^{(*)}}$ ,  $R_{K^{(*)}}$  anomalies in a two-loop radiative neutrino mass model, Phys. Rev. D **102** (2020) no.1, 015019.
- [97] K. S. Babu, P. S. B. Dev, S. Jana and A. Thapa, Unified framework for  $B$ -anomalies, muon  $g-2$  and neutrino masses, JHEP **03** (2021), 179.
- [98] R. Aaij *et al.* [LHCb], Measurement of the  $B_c^-$  meson production fraction and asymmetry in 7 and 13 TeV  $pp$  collisions, Phys. Rev. D **100** (2019) no.11, 112006.
- [99] R. Aaij *et al.* [LHCb], A search for rare  $B \rightarrow D\mu^+\mu^-$  decays, [arXiv:2308.06162 [hep-ex]].
- [100] C. Q. Geng, C. W. Hwang and C. C. Liu, Study of rare  $B_c^+ \rightarrow D_{s,d}^{(*)+} \ell \bar{\ell}$  decays, Phys. Rev. D **65** (2002), 094037.
- [101] W. F. Wang, X. Yu, C. D. Lü and Z. J. Xiao, Semileptonic decays  $B_c^+ \rightarrow D_{(s)}^{(*)}(\ell^+ \nu_\ell, \ell^+ \ell^-, \nu \bar{\nu})$  in the perturbative QCD approach, Phys. Rev. D **90** (2014) no.9, 094018.
- [102] V. V. Kiselev, Exclusive decays and lifetime of  $B_c$  meson in QCD sum rules, [arXiv:hep-ph/0211021 [hep-ph]].
- [103] K. Azizi, F. Falahati, V. Bashiry and S. M. Zebarjad, Analysis of the Rare  $B_c \rightarrow D_{(s,d)}^{(*)} \ell^+ \ell^-$  Decays in QCD, Phys. Rev. D **77** (2008), 114024.
- [104] W. Jaus, Semileptonic Decays of  $B$  and  $D$  Mesons in the Light Front Formalism, Phys. Rev. D **41** (1990), 3394.
- [105] W. Jaus, Semileptonic, radiative, and pionic decays of  $B$ ,  $B^*$  and  $D$ ,  $D^*$  mesons, Phys. Rev. D **53** (1996), 1349 [erratum: Phys. Rev. D **54** (1996), 5904].
- [106] H. Y. Cheng, C. Y. Cheung and C. W. Hwang, Mesonic form-factors and the Isgur-Wise function on the light front, Phys. Rev. D **55** (1997), 1559-1577.
- [107] H. Y. Cheng, C. Y. Cheung, C. W. Hwang and W. M. Zhang, A Covariant light front model of heavy mesons within HQET, Phys. Rev. D **57** (1998), 5598-5610.
- [108] W. Jaus, Covariant analysis of the light front quark model, Phys. Rev. D **60** (1999), 054026 doi:10.1103/PhysRevD.60.054026.
- [109] H. Y. Cheng and C. K. Chua, Covariant light front approach for  $B \rightarrow K^* \gamma, K_1 \gamma, K_2^* \gamma$  decays, Phys. Rev. D **69** (2004), 094007 [erratum: Phys. Rev. D **81** (2010), 059901].
- [110] H. Y. Cheng, C. K. Chua and C. W. Hwang, Covariant light front approach for  $s$ -wave and  $p$ -wave mesons: Its application to decay constants and form-factors, Phys. Rev. D **69** (2004), 074025.
- [111] C. K. Chua, Covariant light front approach for  $s$ -wave and  $p$ -wave mesons, J. Korean Phys. Soc. **45** (2004), S256-S261.
- [112] W. Wang, Y. L. Shen and C. D. Lü, The Study of  $B_c \rightarrow X(3872)\pi^-(K^-)$  decays in the covariant light-front approach, Eur. Phys. J. C **51** (2007), 841-847.
- [113] W. Wang and Y. L. Shen,  $D_s \rightarrow K, K^*, \phi$  form factors in the Covariant Light-Front Approach and Exclusive  $D_s$  Decays, Phys. Rev. D **78** (2008), 054002.
- [114] W. Wang, Y. L. Shen and C. D. Lü, Covariant Light-Front Approach for  $B_c$  transition form factors, Phys. Rev. D **79** (2009), 054012.
- [115] Y. L. Shen and Y. M. Wang,  $J/\psi$  weak decays in the covariant light-front quark model, Phys. Rev. D **78** (2008), 074012.
- [116] X. X. Wang, W. Wang and C. D. Lu,  $B_c$  to  $p$ -wave charmonia transitions in covariant light-front approach, Phys. Rev. D **79** (2009), 114018.
- [117] C. H. Chen, Y. L. Shen and W. Wang,  $|V_{ub}|$  and  $B \rightarrow \eta^{(\prime)}$  Form Factors in Covariant Light Front Approach, Phys. Lett. B **686** (2010), 118-123.
- [118] H. Y. Cheng and C. K. Chua,  $B \rightarrow V, A, T$  tensor form factors in the covariant light-front approach: Implications on radiative  $B$  decays, Phys. Rev. D **81** (2010), 114006 [erratum: Phys. Rev. D **82** (2010), 059904].
- [119] H. M. Choi, Exclusive Rare  $B_s \rightarrow (K, \eta, \eta') \ell^+ \ell^-$  Decays in the Light-Front Quark Model, J. Phys. G **37** (2010), 085005.
- [120] G. Li, F. I. Shao and W. Wang,  $B_s \rightarrow D_s(3040)$  form factors and  $B_s$  decays into  $D_s(3040)$ , Phys. Rev. D **82** (2010), 094031.
- [121] H. M. Choi and C. R. Ji, Light-front dynamic analysis of transition form factors in the process of  $P \rightarrow V \ell \nu_\ell$ , Nucl. Phys. A **856** (2011), 95-111.
- [122] H. W. Ke and X. Q. Li, Vertex functions for  $d$ -wave mesons in the light-front approach, Eur. Phys. J. C **71** (2011), 1776.
- [123] R. C. Verma, Decay constants and form factors of  $s$ -wave and  $p$ -wave mesons in the covariant light-front quark model, J. Phys. G **39** (2012), 025005.
- [124] H. W. Ke, T. Liu and X. Q. Li, Transitions of  $B_c \rightarrow \psi(1S, 2S)$  and the modified harmonic oscillator wave function in LFQM, Phys. Rev. D **89** (2014) no.1, 017501.
- [125] H. Xu, Q. Huang, H. W. Ke and X. Liu, Numerical analysis of the production of  $D^{(*)}(3000)$ ,  $D_{sJ}(3040)$  and their partners through the semileptonic decays of  $B_{(s)}$  mesons in terms of the light front quark model, Phys. Rev. D **90** (2014) no.9, 094017.
- [126] Y. J. Shi, W. Wang and Z. X. Zhao,  $B_c \rightarrow B_{sJ}$  form factors and  $B_c$  decays into  $B_{sJ}$  in covariant light-front approach, Eur. Phys. J. C **76** (2016) no.10, 555.
- [127] K. Chen, H. W. Ke, X. Liu and T. Matsuki, Estimating the production rates of  $D$ -wave charmed mesons via the semileptonic decays of bottom mesons, Chin. Phys. C **43** (2019) no.2,



- 023106.
- [128] H. Y. Cheng and X. W. Kang, Branching fractions of semileptonic  $D$  and  $D_s$  decays from the covariant light-front quark model, *Eur. Phys. J. C* **77** (2017) no.9, 587 [erratum: *Eur. Phys. J. C* **77** (2017) no.12, 863].
  - [129] X. W. Kang, T. Luo, Y. Zhang, L. Y. Dai and C. Wang, Semileptonic  $B$  and  $B_s$  decays involving scalar and axial-vector mesons, *Eur. Phys. J. C* **78** (2018) no.11, 909.
  - [130] Q. Chang, X. N. Li, X. Q. Li, F. Su and Y. D. Yang, Self-consistency and covariance of light-front quark models: testing via  $P$ ,  $V$  and  $A$  meson decay constants, and  $P \rightarrow P$  weak transition form factors, *Phys. Rev. D* **98** (2018) no.11, 114018.
  - [131] Q. Chang, Y. Zhang and X. Li, Study of  $\bar{B}_{u,d,s}^* \rightarrow D_{u,d,s}^* V$  ( $V = D_{d,s}^{*-}, K^{*-}, \rho^-$ ) weak decays, *Chin. Phys. C* **43** (2019) no.10, 103104.
  - [132] Q. Chang, L. T. Wang and X. N. Li, Form factors of  $V' \rightarrow V''$  transition within the light-front quark models, *JHEP* **12** (2019), 102.
  - [133] Q. Chang, X. N. Li and L. T. Wang, Revisiting the form factors of  $P \rightarrow V$  transition within the light-front quark models, *Eur. Phys. J. C* **79** (2019) no.5, 422.
  - [134] Q. Chang, X. L. Wang, J. Zhu and X. N. Li, Study of  $b \rightarrow c$  induced  $\bar{B}^* \rightarrow V \ell \bar{\nu}_\ell$  decays, *Adv. High Energy Phys.* **2020** (2020), 3079670.
  - [135] Q. Chang, X. L. Wang and L. T. Wang, Tensor form factors of  $P \rightarrow P, S, V$  and  $A$  transitions within standard and covariant light-front approaches, *Chin. Phys. C* **44** (2020) no.8, 083105.
  - [136] H. M. Choi, Self-consistent light-front quark model analysis of  $B \rightarrow D \ell \bar{\nu}_\ell$  transition form factors, *Phys. Rev. D* **103** (2021) no.7, 073004.
  - [137] H. M. Choi, Current-Component Independent Transition Form Factors for Semileptonic and Rare  $D \rightarrow \pi K$  Decays in the Light-Front Quark Model, *Adv. High Energy Phys.* **2021** (2021), 4277321.
  - [138] L. Chen, Y. W. Ren, L. T. Wang and Q. Chang, Form factors of  $P \rightarrow T$  transition within the light-front quark models, *Eur. Phys. J. C* **82** (2022) no.5, 451.
  - [139] A. J. Arifi, H. M. Choi, C. R. Ji and Y. Oh, Independence of current components, polarization vectors, and reference frames in the light-front quark model analysis of meson decay constants, *Phys. Rev. D* **107** (2023) no.5, 053003.
  - [140] Z. Q. Zhang, Z. J. Sun, Y. C. Zhao, Y. Y. Yang and Z. Y. Zhang, Covariant light-front approach for  $B_c$  decays into charmonium: implications on form factors and branching ratios, *Eur. Phys. J. C* **83** (2023) no.6, 477.
  - [141] Y. J. Shi and Z. P. Xing, Heavy flavor conserved semileptonic decay of  $B_s$  in the covariant light-front approach, [[arXiv:2307.02767](#) [hep-ph]].
  - [142] A. Hazra, T. M. S., N. Sharma and R. Dhir,  $B_c$  to  $A$  Transition Form Factors and Semileptonic Decays in Self-consistent Covariant Light-front Approach, [[arXiv:2309.03655](#) [hep-ph]].
  - [143] H. W. Ke, X. Q. Li and Z. T. Wei, Diquarks and  $\Lambda_b \rightarrow \Lambda_c$  weak decays, *Phys. Rev. D* **77** (2008), 014020.
  - [144] H. W. Ke, X. H. Yuan, X. Q. Li, Z. T. Wei and Y. X. Zhang,  $\Sigma_b \rightarrow \Sigma_c$  and  $\Omega_b \rightarrow \Omega_c$  weak decays in the light-front quark model, *Phys. Rev. D* **86** (2012), 114005.
  - [145] H. W. Ke, N. Hao and X. Q. Li,  $\Sigma_b \rightarrow \Sigma_c^*$  weak decays in the light-front quark model with two schemes to deal with the polarization of diquark, *J. Phys. G* **46** (2019) no.11, 115003.
  - [146] W. Wang, F. S. Yu and Z. X. Zhao, Weak decays of doubly heavy baryons: the  $1/2 \rightarrow 1/2$  case, *Eur. Phys. J. C* **77** (2017) no.11, 781.
  - [147] J. Zhu, Z. T. Wei and H. W. Ke, Semileptonic and nonleptonic weak decays of  $\Lambda_b^0$ , *Phys. Rev. D* **99** (2019) no.5, 054020.
  - [148] Z. X. Zhao, Weak decays of heavy baryons in the light-front approach, *Chin. Phys. C* **42** (2018) no.9, 093101.
  - [149] Z. P. Xing and Z. X. Zhao, Weak decays of doubly heavy baryons: the FCNC processes, *Phys. Rev. D* **98** (2018) no.5, 056002.
  - [150] C. K. Chua, Color-allowed bottom baryon to charmed baryon nonleptonic decays, *Phys. Rev. D* **99** (2019) no.1, 014023.
  - [151] Z. X. Zhao, Weak decays of doubly heavy baryons: the  $1/2 \rightarrow 3/2$  case, *Eur. Phys. J. C* **78** (2018) no.9, 756.
  - [152] C. K. Chua, Color-allowed bottom baryon to  $s$ -wave and  $p$ -wave charmed baryon nonleptonic decays, *Phys. Rev. D* **100** (2019) no.3, 034025.
  - [153] H. W. Ke, F. Lu, X. H. Liu and X. Q. Li, Study on  $\Xi_{cc} \rightarrow \Xi_c$  and  $\Xi_{cc} \rightarrow \Xi_c'$  weak decays in the light-front quark model, *Eur. Phys. J. C* **80** (2020) no.2, 140.
  - [154] H. W. Ke, N. Hao and X. Q. Li, Revisiting  $\Lambda_b \rightarrow \Lambda_c$  and  $\Sigma_b \rightarrow \Sigma_c$  weak decays in the light-front quark model, *Eur. Phys. J. C* **79** (2019) no.6, 540.
  - [155] X. H. Hu, R. H. Li and Z. P. Xing, A comprehensive analysis of weak transition form factors for doubly heavy baryons in the light front approach, *Eur. Phys. J. C* **80** (2020) no.4, 320.
  - [156] C. Q. Geng, C. C. Lih, C. W. Liu and T. H. Tsai, Semileptonic decays of  $\Lambda_c^+$  in dynamical approaches, *Phys. Rev. D* **101** (2020) no.9, 094017.
  - [157] Y. K. Hsiao, L. Yang, C. C. Lih and S. Y. Tsai, Charmed  $\Omega_c$  weak decays into  $\Omega$  in the light-front quark model, *Eur. Phys. J. C* **80** (2020) no.11, 1066.
  - [158] Y. K. Hsiao and C. C. Lih, Fragmentation fraction  $f_{\Omega_b}$  and the  $\Omega_b \rightarrow \Omega J/\psi$  decay in the light-front formalism, *Phys. Rev. D* **105** (2022) no.5, 056015.
  - [159] C. Q. Geng, C. W. Liu and T. H. Tsai, Non-leptonic two-body decays of  $\Lambda_b^0$  in light-front quark model, *Phys. Lett. B* **815** (2021), 136125.
  - [160] H. W. Ke, Q. Q. Kang, X. H. Liu and X. Q. Li, Weak decays of in the light-front quark model \*, *Chin. Phys. C* **45** (2021) no.11, 113103.
  - [161] Z. X. Zhao, Weak decays of triply heavy baryons: the  $3/2 \rightarrow 1/2$  case, [[arXiv:2204.00759](#) [hep-ph]].
  - [162] C. Q. Geng, C. W. Liu, Z. Y. Wei and J. Zhang, Weak radiative decays of antitriplet bottomed baryons in light-front quark model, *Phys. Rev. D* **105** (2022) no.7, 073007.
  - [163] W. Wang and Z. P. Xing, Weak decays of triply heavy baryons in light front approach, *Phys. Lett. B* **834** (2022), 137402.
  - [164] H. Liu, W. Wang and Z. P. Xing, Baryonic heavy-to-light form factors induced by tensor current in light-front approach, [[arXiv:2305.01168](#) [hep-ph]].
  - [165] F. Lu, H. W. Ke, X. H. Liu and Y. L. Shi, Study on the weak decay between two heavy baryons  $\mathcal{B}_i(\frac{1}{2}^+) \rightarrow \mathcal{B}_f(\frac{3}{2}^+)$  in the light-front quark model, *Eur. Phys. J. C* **83** (2023) no.5, 412.
  - [166] Z. X. Zhao, F. W. Zhang, X. H. Hu and Y. J. Shi, Baryons in the light-front approach: The three-quark picture, *Phys. Rev. D* **107** (2023) no.11, 116025.
  - [167] Y. S. Li, X. Liu and F. S. Yu, Revisiting semileptonic decays of  $\Lambda_{b(c)}$  supported by baryon spectroscopy, *Phys. Rev. D* **104** (2021) no.1, 013005.
  - [168] Y. S. Li and X. Liu, Restudy of the color-allowed two-body nonleptonic decays of bottom baryons  $\Xi_b$  and  $\Omega_b$  supported by hadron spectroscopy, *Phys. Rev. D* **105** (2022) no.1, 013003.
  - [169] Y. S. Li, S. P. Jin, J. Gao and X. Liu, Transition form factors and angular distributions of the  $\Lambda_b \rightarrow \Lambda(1520)(\rightarrow N \bar{K}) \ell^+ \ell^-$  decay supported by baryon spectroscopy, *Phys. Rev. D* **107** (2023) no.9, 093003.
  - [170] Y. S. Li and X. Liu, Investigating the transition form factors of  $\Lambda_b \rightarrow \Lambda_c(2625)$  and  $\Xi_b \rightarrow \Xi_c(2815)$  and the corresponding



- weak decays with support from baryon spectroscopy, Phys. Rev. D **107** (2023) no.3, 033005.
- [171] G. Buchalla, A. J. Buras and M. E. Lautenbacher, Weak decays beyond leading logarithms, Rev. Mod. Phys. **68** (1996), 1125-1144.
  - [172] R. L. Workman *et al.* [Particle Data Group], Review of Particle Physics, PTEP **2022** (2022), 083C01.
  - [173] C. H. Chen and C. Q. Geng, Baryonic rare decays of  $\Lambda_b \rightarrow \Lambda \ell^+ \ell^-$ , Phys. Rev. D **64** (2001), 074001.
  - [174] M. J. Aslam, Y. M. Wang and C. D. Lü, Exclusive semileptonic decays of  $\Lambda_b \rightarrow \Lambda \ell^+ \ell^-$  in supersymmetric theories, Phys. Rev. D **78** (2008), 114032.
  - [175] G. M. Asatryan and A. Ioannisian, CP violation in the decay  $b \rightarrow s \gamma$  in the left-right symmetric model, Phys. Rev. D **54** (1996), 5642-5646.
  - [176] A. J. Buras and M. Munz, Effective Hamiltonian for  $B \rightarrow X_s e^+ e^-$  beyond leading logarithms in the NDR and HV schemes, Phys. Rev. D **52** (1995), 186-195.
  - [177] A. Khodjamirian, T. Mannel, A. A. Pivovarov and Y. M. Wang, Charm-loop effect in  $B \rightarrow K^{(*)} \ell^+ \ell^-$  and  $B \rightarrow K^* \gamma$ , JHEP **09** (2010), 089.
  - [178] A. Khodjamirian, T. Mannel and Y. M. Wang,  $B \rightarrow K \ell^+ \ell^-$  decay at large hadronic recoil, JHEP **02** (2013), 010.
  - [179] W. Altmannshofer, P. Ball, A. Bharucha, A. J. Buras, D. M. Straub and M. Wick, Symmetries and Asymmetries of  $B \rightarrow K^* \mu^+ \mu^-$  Decays in the Standard Model and Beyond, JHEP **01** (2009), 019.
  - [180] Y. Li and C. D. Lü, Recent Anomalies in B Physics, Sci. Bull. **63** (2018), 267-269.
  - [181] M. Wirbel, B. Stech and M. Bauer, Exclusive Semileptonic Decays of Heavy Mesons, Z. Phys. C **29** (1985), 637.
  - [182] P. Ball and V. M. Braun, Exclusive semileptonic and rare B meson decays in QCD, Phys. Rev. D **58** (1998), 094016.
  - [183] A. Ali, P. Ball, L. T. Handoko and G. Hiller, A Comparative study of the decays  $B \rightarrow (K, K^*) \ell^+ \ell^-$  in standard model and supersymmetric theories, Phys. Rev. D **61** (2000), 074024.
  - [184] X. J. Li, Y. S. Li, F. L. Wang and X. Liu, Whole  $B_c$  meson spectroscopy under the unquenched picture, [arXiv:2308.07206 [hep-ph]].
  - [185] R. Dhir and R. C. Verma,  $B_c$  Meson Form-factors and  $B_c \rightarrow PV$  Decays Involving Flavor Dependence of Transverse Quark Momentum, Phys. Rev. D **79** (2009), 034004.